Stark broadening of hydrogen lines in plasmas

V. S. Lisitsa

Usp. Fiz. Nauk 122, 449–495 (July 1977)

The results of theoretical and experimental studies of the Stark broadening of hydrogen lines in plasmas made during the last 10–15 years are reviewed. Plasmas and the hydrogen atom are the objects in which specific features of the Coulomb interaction manifest themselves most clearly. The statistics of the Coulomb microfield produced by the ions and electrons in a plasma (with allowance for the effects of screening and ion-ion correlations) and the temporal fluctuations of that microfield are discussed briefly. The dynamics of the interaction of the plasma microfield with the radiating atom is analyzed in detail. In addition to discussing the well known approximations in the theory of line broadening–the impact and statistical approximations–considerable attention is given to the intermediate spectral region in which both those approximations break down. The possibility of describing this region is due to a specific (four-dimensional) symmetry of the hydrogen atom, which makes it possible to find accurate wave functions for the atom in the field of the charged particle responsible for the broadening. The accurate solution is used to analyze the transition from electron-impact broadening to statistical broadening in the wing of the line. Considerable attention is given to the thermal motion of the ions and the related "reduced mass effect" that manifests itself at the centers of the Balmer lines. The basic experimental results that make it possible to test the conclusions of existing theory and to discern new problems are presented. The quantum formulation of the line-broadening problem is discussed, as well as line broadening for hydrogenlike ions.

PACS numbers: 52.25.Ps, 32.60.+i

CONTENTS

1. INTRODUCTION

For almost sixty years, since the appearance of the fundamental paper by Holtsmark,[1] the problem of the Stark broadening of hydrogen lines in plasma has attracted the attention of physicists. This interest has continued not only because the question is of practical importance for plasma diagnostics, but also because it involves two objects (the hydrogen atom and the plasma) for which the specific features of the long-range Coulomb interaction are particularly well defined. Since the hydrogen atom is the simplest quantum-mechanical system, it is clear that broadening is among the few practical problems for which relatively simple and, at the same time, rigorous models can be constructed. Moreover, these models admit of a direct experimental verification. The accuracy of modern plasma experiments is very high, namely, between 1% and 10%.

The theory of line broadening includes a range of problems from atomic spectroscopy, the theory of atomic collisions, and the statistics of the fluctuating plasma microfield. Its task is to investigate the dependence of the line profile $I(\omega)$ radiated (or absorbed) by an atom in plasma on the parameters of the ambient medium. These parameters are the concentration N of particles, the velocity v_e of electrons, the velocity v_i of ions, the electric and magnetic fields in plasma, and so on. One of the important parameters of the line profile itself is the detuning $\Delta\omega$ of the observed frequency ω from the unperturbed frequency ω_0 of the atom ($\Delta\omega = \omega - \omega_0$).

The information that can be extracted from observations on Stark line profiles is of twofold interest. Firstly, measurements of $I(\omega)$ can be used to determine the properties of the surrounding plasma without the use of probes or other objects that distort its properties. Secondly, detailed studies of the line profiles enrich our understanding of the statistics of the fluctuating Coulomb microfield in plasma and the dynamics of its interaction with the atom, and this is of general interest in physics.

The publication of the present review is connected with the completion of a definite stage in the development of the theory of broadening, i.e., direct verification of the theory is now possible because of improvements in experimental procedures. Our aim in this review will be to achieve clarity rather than rigor. The point is that

 0038-5670/77/2007-0603$01.10

recent years have seen a substantial increase in the number of theoretical approaches to the problem of broadening. For example, there is the kinetic equation method,[2] the "relaxation" theory,[3,4] the method of Green's function,[5] the projection operator technique,[6] and so on. We shall not discuss all these possible methods of the theory of broadening, and will confine our attention to the main theoretical and experimental results obtained in this field during the last few years. Readers interested in the history of the problem are referred to the book by Breene.[7] Experimental aspects are discussed in the book by Griem[8] and the review by Wiese.[9] A clear exposition of the fundamentals of the theory of broadening is given by Sobel'man.[10] There are also reviews by Baranger[11] and Traving.[12]

Consider a hydrogen line produced as a result of a dipole transition from an upper (a) to a lower (b) level. Each level of the hydrogen atom with principal quantum number n has n^2 degenerate states.[1)] These states will be labeled α, α' and β, β' for the upper and lower levels, respectively. The fundamental formula of the theory of broadening is the expression for the line profile $I_{ab}(\omega)$ radiated by an atom[8,10]:

$$I_{ab}(\omega)=\frac{1}{\pi}\operatorname{Re}\int_0^\infty e^{-i\omega\tau}K_{ab}(\tau)\,d\tau, \tag{1.1}$$

where the correlation function for the dipole moments of the atom is given by

$$K_{ab}(\tau)=\Big\{\sum_{\alpha,\beta,\sigma}\langle\psi_\alpha(\tau)\,|\,d_\sigma\,|\,\psi_\beta(\tau)\rangle\langle\psi_\beta(0)\,|\,d_\sigma\,|\,\psi_\alpha(0)\rangle\Big\}. \tag{1.2}$$

d_σ is the component of the dipole moment of the atom, ψ_α, ψ_β are the wave functions of the upper and lower states, respectively, and $\{\ldots\}$ represents averaging over the ensemble of perturbing plasma particles. The wave functions ψ_α, ψ_β of the atom in the medium depend on the variables of the plasma.

It is assumed in (1.1) and (1.2) that the only reason for broadening is the interaction between the atom and the plasma particles. This interaction generates the wave functions of the upper and lower states between which the spontaneous transition due to the interaction with the radiation field subsequently takes place. The wave functions $\psi(t)$ satisfy the Schrödinger equation with the following Hamiltonian:

$$\hat{\mathcal{H}}(t)=\hat{\mathcal{H}}_0+\hat{V}(t)=\hat{\mathcal{H}}_0+\mathbf{d}\,[\mathbf{F}_i(t)+\mathbf{F}_e(t)], \tag{1.3}$$

where $\hat{\mathcal{H}}_0$ is the unperturbed Hamiltonian and $\hat{V}(t)$ is the interaction between the atomic dipole moment $\mathbf{d}$ and the electric fields $\mathbf{F}_i(t)$ and $\mathbf{F}_e(t)$ of the plasma ions and electrons. The motion of these charged particles will be assumed to be classical and rectilinear, so that the field $\mathbf{F}(t)$ due to an individual particle will be

$$\mathbf{F}(t)=e\frac{\mathbf{r}_0+\mathbf{v}t}{|\mathbf{r}_0+\mathbf{v}t|^3}=e\frac{\boldsymbol{\rho}+v(t-t_0)}{[\rho^2+v^2(t-t_0)^2]^{3/2}}, \tag{1.4}$$

where $\mathbf{r}_0$ is the position vector and $\mathbf{v}$ the velocity of the particle. It is convenient to express $\mathbf{r}_0$ in terms of the cylindrical coordinates with the z axis parallel to $\mathbf{v}$: $\mathbf{r}_0=\boldsymbol{\rho}-\mathbf{v}t_0$, where $\boldsymbol{\rho}$ is the impact parameter ($\boldsymbol{\rho}\perp\mathbf{v}$) and t_0 is the time of closest approach between the particle and the atom.

The fields $\mathbf{F}_i(t)$ and $\mathbf{F}_e(t)$ are vector sums of fields due to individual particles, so that, for example,

$$\mathbf{F}_i(t)=-e\sum_{k=1}^{\mathcal{N}}\frac{\mathbf{r}_{0k}+\mathbf{v}_kt}{|\mathbf{r}_{0k}+\mathbf{v}_kt|^3}, \tag{1.5}$$

where $\mathcal{N}$ is the total number of ions in the plasma volume V. The particle density $N=\mathcal{N}/V$ will henceforth be assumed to be a given constant.

It is important to note that broadening processes are due to transitions between states belonging to a given level with a fixed principal quantum number n (i.e., the so-called "isoenergetic surface"). This means that transitions between levels a and b due to interactions with the plasma particles can be neglected. It follows that broadening processes correspond to a small energy transfer between the excited atom and the broadening particles. This energy is of the order of the observed spectral interval $\hbar\Delta\omega$ and is usually much less than the temperature kT of the plasma.

It is clear from the foregoing discussion that the dipole moment d of the hydrogen atom appears in the theory of broadening in two ways. Firstly, the matrix elements of d between the levels a and b determine the interaction between the atom and the radiation field. Secondly, for states with given n, the operator d determines the interaction between the atom and the plasma microfield.

The broadening problem can be divided into two parts in a natural fashion. Thus, we have the dynamic part connected with the solution of the Schrödinger equation (1.3) for the atom in the variable electric fields, and the static part connected with averaging of the resulting solution over the ensemble of perturbing plasma particles. These two problems cannot be solved in a general form, and a number of approximations are used to determine the spectrum. These are considered below.

2. THE "OLD" ADIABATIC THEORY OF BROADENING

Let us begin by considering the fundamentals of the broadening process in terms of the simple adiabatic model put forward by Weisskopf[13] and then improved by Lindholm.[14] We shall assume that the hydrogen line broadening is due to charged particles of a single type. The atomic levels then undergo[15] the Stark frequency splitting given by

$$\varkappa=\frac{C}{e}F=\frac{3}{2}n(n_1-n_2)\frac{\hbar}{me}F, \tag{2.1}$$

where C is the Stark constant for the component with parabolic quantum numbers n_1, n_2 corresponding to the level n, and F is the electric field strength due to the charged particles.

[1)] The spin of the electron will be ignored throughout, because Stark broadening is usually greater than the fine structure of levels.

The adiabatic model rests on the assumption that the interaction between the atom and the field $F(t)$ leads only to a change in the phase of the wave function (phase modulation)

$$\psi_a(t) \propto \exp\left[i\int_0^t \varkappa_a(\tau)\,d\tau\right]. \tag{2.2}$$

It is clear that, according to (1.2), the correlation function in this approximation takes the form

$$K(\tau)=\left\langle \exp\left[i\int_0^\tau \varkappa(t)\,dt\right]\right\rangle. \tag{2.3}$$

We shall assume that the perturbation $\varkappa(t)$ is due to a single perturbing particle closest to the atom. The phase shift produced during the complete transit of the particle between $t=-\infty$ and $t=+\infty$ is then given by

$$\Delta\varphi=\int_{-\infty}^{\infty}\varkappa(t)\,dt=\int_{-\infty}^{\infty}\frac{C\,dt}{\rho^2+v^2(t-t_0)^2}=\pi\frac{C}{\rho v}. \tag{2.4}$$

The phase change $\Delta\varphi$ characterizes the effectiveness of the collision. In fact, coherence is totally "lost" when $\Delta\varphi\sim\pi$, and the atom "forgets" the initial phase value after this type of collision. The impact parameter ρ_W for which $\Delta\varphi\sim\pi$ is called the *Weisskopf radius* and is given by

$$\rho_W\sim\frac{C}{v}. \tag{2.5}$$

This radius determines the effective cross section $\sigma_W\sim\pi\rho_W^2$, which corresponds to the loss of coherence and is called the optical cross section for collisions. An important quantity in this context is the Weisskopf collision frequency (or the reciprocal of the collision time)

$$\Omega\sim\frac{v}{\rho_W}=\frac{v^2}{C}. \tag{2.6}$$

The Weisskopf radius defines a certain effective interaction volume which is of the order of ρ_W^3. When the particle density is N, the number of particles found on average within this volume is

$$N\rho_W^3\equiv g\ . \tag{2.7}$$

It follows that, when $g\gg1$, a large number of particles interact simultaneously with the atom. If, on the other hand, $g\ll1$, only one (nearest) particle is involved in the interaction. Consequently, the parameter g provides a measure of the extent to which the broadening collisions may be regarded as binary.

The characteristic time between collisions is determined by the collision frequency (or the reciprocal of the time for one mean free path)

$$\gamma\sim Nv\sigma_W\sim\frac{NC^2}{v}. \tag{2.8}$$

We note that the ratio of the characteristic frequencies Ω and γ is also equal to the parameter g, i.e., $\gamma/\Omega=g$.

We now follow Anderson[16] and assume that the shift $\varkappa$ in (2.3) is the sum of the shifts $\varkappa_k$ due to the individual particles[2)]

$$\varkappa(t)=\sum_{k=1}^{\mathcal{N}}\varkappa_k(t). \tag{2.9}$$

If the particles are independent, the resultant correlation function splits into the product of functions corresponding to the individual particles:

$$K(\tau)=\left\langle \exp\left[i\sum_{k=1}^{\mathcal{N}}\int_0^\tau \varkappa_k(t)\,dt\right]\right\rangle_{\mathcal{N}}=\left\langle\prod_{k=1}^{\mathcal{N}}\exp\left[i\int_0^\tau\varkappa_k(t)\,dt\right]\right\rangle_{\mathcal{N}}=\left\langle\exp\left[i\int_0^\tau\varkappa(t)\,dt\right]\right\rangle_1^{\mathcal{N}},$$

where $\langle\cdots\rangle_{\mathcal{N}}$ represents averaging over the phase volume of all the $\mathcal{N}$ particles and $\langle\cdots\rangle_1$ corresponds to averaging over the phase volume of one particle. The latter includes integration with respect to the coordinates $d\mathbf{r}_0/V$ and over the velocity distribution $f(v)dv$ of the particles:

$$K(\tau)=\left\{\left[1-\frac{1}{V}\int d\mathbf{r}_0\int dv\,f(v)\right]\left[1-\exp\left(i\int_0^\tau\varkappa(t)\,dt\right)\right]\right\}^{\mathcal{N}=NV}.$$

If we pass to the limit as $\mathcal{N}\to\infty$, $V\to\infty$ with $N=\mathcal{N}/V=\text{const}$, we obtain

$$K(\tau)=e^{-NV(\tau)}, \tag{2.10}$$

where the "collision volume" is given by

$$V(\tau)=\int d\mathbf{r}\,f(v)\int_0^\infty 2\pi\rho\,d\rho\int_{-\infty}^{\infty}dz\left\{1-\exp\left(i\int_z^{z+v\tau}\frac{C}{\rho^2+u^2}\frac{du}{v}\right)\right\} \tag{2.11}$$

(we have transformed to the cylindrical coordinates: $d\mathbf{r}_0=2\pi\rho\,d\rho\,dz$). We shall now assume, for simplicity, that the velocity v is fixed and is equal to some characteristic velocity corresponding to the Maxwellian velocity distribution $f(v)$.

It is clear from (2.11) that the imaginary part, $\mathrm{Im}V(\tau)$, diverges linearly for large values of ρ, which is connected with the specific character of the long-range Coulomb interaction $\varkappa=C/r^2$. This divergence is not physically meaningful and, as will be seen below, is unimportant in the more rigorous approach. In fact, we have ignored the symmetry of Stark splitting which is reflected in the fact that the quantity C in (2.1) can assume positive and negative values with equal probability. The terms that are odd in C in the expression for $\mathrm{Im}V(\tau)$ are, in fact, zero and it will be sufficient for us to confine our attention to $\mathrm{Re}V(\tau)$.

It is readily seen that the only time scale for a change in the collision volume $V(\tau)$ is the reciprocal of the Weisskopf frequency Ω^{-1}. There are, therefore, two characteristic frequency ranges, namely, $\Omega\tau\ll1$ and $\Omega\tau\gg1$. For small times, we have from (2.11)

[2)] This "scalar" model of the addition of perturbations is valid only for a hydrogen atom in the binary region, in which $g\ll1$; see below.

$$\mathrm{Re}\,V(\tau)=\int_0^\infty 4\pi r_0^2\,dr_0\,[1-\cos(C\tau/r_0^2)]=\frac{8}{3}(\pi C\tau)^{3/2},\quad \Omega\tau\ll 1. \tag{2.12}$$

For large times, $\Omega\tau\gg 1$,

$$\mathrm{Re}\,V(\tau)\approx V'(\infty)\,\tau=v\sigma_W\tau, \tag{2.13}$$

where the derivative of the collision volume $V'(\infty)$ is given by

$$V'(\infty)=v2\pi\int_0^{\rho_m}\rho\,d\rho\left[1-\cos\left(\frac{C}{v}\int_{-\infty}^{\infty}\frac{du}{\rho^2+u^2}\right)\right]=2\pi^3\frac{C^2}{v}\ln\frac{\rho_m}{\rho_W}. \tag{2.14}$$

We have introduced an upper cutoff limit ρ_m for the logarithmically divergent integral with respect to ρ. We shall choose ρ_m below.

It is important to note here that when $\Omega\tau\gg 1$ the evolution of the collision volume depends on the Weisskopf cross section σ_W, which is determined by the integral over the entire time of flight between $t=-\infty$ and $t=+\infty$, i.e., it is determined by completed transits. The region $\Omega\tau\gg 1$, which corresponds to fast collisions (large Ω), is called the *impact* region. It is clear from (2.14) that the main contribution to the latter is provided by distant (weak) transits with $\rho\gg\rho_W\sim C/v$, and this is logarithmically large in comparison with the contribution of "strong" collisions with $\rho\lesssim\rho_W$.

The result given by (2.12) for $\Omega\tau\ll 1$ is independent of velocity and is wholly connected with the form of the static interaction potential C/r_0^2. This region is, therefore, frequently referred to as the static region.[3)]

We now consider the case of binary (two-body) collisions $g\ll 1$ and examine[17] the transition between the impact and static regions within the line profile $I(\omega)$. This can be done by substituting (2.10) in (1.1) and integrating by parts:

$$I(\omega)=\frac{1}{\pi}\mathrm{Re}\left[-\frac{1}{i\Delta\omega}+\frac{N}{i\Delta\omega}\int_0^\infty d\tau e^{-i\Delta\omega\tau}V'(\tau)\,e^{-NV(\tau)}\right]. \tag{2.15}$$

As already noted, the characteristic scale for a change in the functions $V(\tau)$ and $V'(\tau)$ is Ω^{-1}. Let us transform (2.15) by adding to $V'(\tau)$ the value of $V'(\infty)$ and then subtracting the same quantity from it. One of the resulting integrals reduces to $I(\omega)$ and, in the other, we can set $\exp[-NV(\tau)]\approx 1$. The integrand in this integral then contains the difference $V'(\tau)-V'(\infty)$, which vanishes for $\tau\gtrsim\Omega^{-1}$. However, the value of $NV(\tau)$ is small in this region: $N|V(\tau\sim\Omega^{-1})|\lesssim N|V'(\infty)|\Omega^{-1}=g\ll 1$, the last part of which is, of course, the definition of a binary encounter. Simple rearrangement then enables us to express the line profile $I(\omega)$ in the following form:

$$I(\omega)=\frac{1}{\pi}\frac{\gamma(\omega)}{\Delta\omega^2+\gamma^2(\omega)}, \tag{2.16}$$

$$\gamma(\omega)=N\,\mathrm{Re}\int_0^\infty d\tau e^{i\Delta\omega\tau}V''(\tau)=\pi Nv\int_0^\infty d\rho\,\rho\left|\int_{-\infty}^{\infty}dt\,\varkappa(t)\exp\left[i\Delta\omega t-i\int_0^t d\tau\,\varkappa(\tau)\right]\right|^2. \tag{2.17}$$

[3)] This seems to us to be more appropriate than the frequently used "quasistatic" or the earlier designation "statistical."

These expressions lead to the following very interesting conclusion: the line profile in the case of the binary approximation ($g\ll 1$) has the structure of the Lorentz formula with a "variable width" $\gamma(\omega)$. This result was obtained by Yakimets[5] for a more general (nonadiabatic) case by the method of Green functions. The characteristic scale of a change in the function $\gamma(\omega)$ is, clearly, the Weisskopf frequency Ω.

It follows that a smooth variation of the collision volume $V(\tau)$ from small values to large values of τ corresponds to a smooth variation in the "variable width" $\gamma(\omega)$ from large values to small values of $\Delta\omega$. This, in turn, corresponds to the "uncertainty relation" for a Fourier inversion: $\Delta\omega\tau_{eff}\sim 1$.

The foregoing discussion provides a clear description of the nature of the spectrum for small ($\Delta\Omega\ll\Omega$) and large ($\Delta\omega\gg\Omega$) frequency detuning. In fact, (2.17) yields the following order-of-magnitude expression: $\gamma(\omega)\sim N\,\mathrm{Re}V'(\tau_{eff})$. Since $\tau_{eff}\sim\Delta\omega^{-1}$, (2.12) and (2.13) yield $\gamma(\Delta\omega\gg\Omega)\propto NC^{3/2}\tau_{eff}^{1/2}\propto NC^{3/2}\Delta\omega^{-1/2}$ and $\gamma(\Delta\omega\ll\Omega)\propto Nv\sigma_W\equiv\gamma(0)$. Substituting these values of $\gamma(\omega)$ in (2.16), we obtain

$$I(\omega)\approx\begin{cases}\dfrac{1}{\pi}\dfrac{\gamma(0)}{\Delta\omega^2+\gamma^2(0)}, & \Delta\omega\ll\Omega,\\ \dfrac{2\pi NC^{3/2}}{\Delta\omega^{5/2}}, & \Delta\omega\gg\Omega.\end{cases} \tag{2.18}$$

The two regions $\Delta\omega\ll\Omega$ and $\Delta\omega\gg\Omega$ are commonly referred to as the impact and static regions. This terminology is adopted because the line profile given by (2.18) for $\Delta\omega\ll\Omega$ has the structure of the (impact) Lorentz formula with constant width $\gamma(\omega)\approx\gamma(0)$, but, for $\Delta\omega\gg\Omega$, it does not depend on the particle velocity (static case).

For a more detailed analysis of the profile (in particular, the case where $\Delta\omega\sim\Omega$), it is convenient to introduce the dimensionless frequency $x=\Delta\omega/\Omega$ and the dimensionless line profile $I(x)$ defined by $I(x)dx=I(\omega)d\omega$. It then follows from (2.16) that

$$I(x)=\frac{1}{\pi}\frac{g\gamma(x)}{x^2+g^2\gamma^2(x)}. \tag{2.19}$$

The dimensionless width $\gamma(x)$ can easily be found from (2.17). If we take the specific interaction $\varkappa(t)=C/C\rho^2+v^2t^2)$ and substitute $\varphi=\arctan(vt/\rho)$, we obtain an analytic expression for $\gamma(x)$ in terms of the confluent hypergeometric function $W_{\lambda,\mu}(z)$ (the Whittaker function,[18] p. 419)

$$\gamma(x)=\pi\int_0^\infty\frac{dy}{y}k_{1/y}^2(2xy),\qquad k_\nu(z)=\int_0^\pi d\varphi\cos(z\,\mathrm{tg}\,\varphi-\nu\varphi)=\frac{W_{\nu/2,\,1/2}(2z)}{\Gamma(1+\nu/2)} \tag{2.20}$$

where $\Gamma(z)$ is the gamma function. We note that the existence of the analytic expression (2.20) is also connected with the specific properties of hydrogen.

The limiting values of $\gamma(x)$ are as follows:

$$\gamma(x)\approx\begin{cases}-\pi^3[\ln x+C]\equiv\gamma_{\mathrm{imp}}, & x\ll 1,\\ \dfrac{2\pi^2}{\sqrt{x}}\equiv\gamma_{\mathrm{stat}}(x), & x\gg 1.\end{cases} \tag{2.21}$$

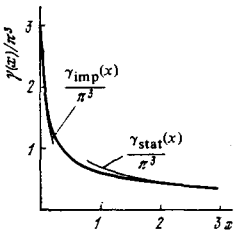

FIG. 1. "Variable linewidth" $\gamma(x)$ and its impact and static limits $\gamma_{\text{imp}}(x)$ and $\gamma_{\text{stat}}(x)$.

Substitution of (2.21) into (2.19) yields, of course, the expression given by (2.18).

Figure 1 shows a graph of $\gamma(x)$ calculated[19] from (2.20) together with its limiting values (2.21).

Let us now consider the properties of the profile for both ranges of values of $\Delta\omega$. In the impact region ($\Delta\omega \ll \Omega$), the linewidth diverges logarithmically as $\Delta\omega$ (or x) $\to 0$. This divergence corresponds to the divergence of the collision volume (2.14) for $\rho_m \to \infty$. In fact, there is always an upper cutoff parameter in plasma. It is equal to the Debye shielding length

$$\rho_D = \sqrt{\frac{kT}{4\pi N e^2}}. \tag{2.22}$$

It follows that, at any rate, $\rho_m \lesssim \rho_D$. We note, however, that the width $\gamma(\omega)$ is finite for finite values of $\Delta\omega$ and, according to (2.21), the logarithm contains the ratio of the two lengths $\rho_\omega \sim v/\Delta\omega$ and $\rho_W \sim C/v$. It follows that, in addition to ρ_D, there is a further cutoff parameter, namely, $\rho_\omega \sim v/\Delta\omega$. This was introduced by Lewis[20] (see also Kogan[21]). The existence of this parameter is connected wholly with the long-range character of the Coulomb interaction. The particular feature of this interaction is that, strictly speaking, the impact parameter is not valid for it since it involves completed transits between $t = -\infty$ and $t = +\infty$. Thus, more rigorous analysis of the collision volume $V(\tau)$ for $\tau \to \infty$ would show that, for large (but finite) values of τ, we have $V'(\tau) \propto \ln(v\tau/\rho_W)$, which corresponds to $\rho_m \sim v\tau$ in (2.14). This means that the only transits that can be regarded as completed for finite τ are those with $\rho \leq v\tau$. This was first pointed out by Kogan.[22] In the theory of broadening, finite $\Delta\omega$ always correspond to finite τ: $\tau_{\text{eff}} \sim \Delta\omega^{-1}$. Hence, it is clear that the Lewis cutoff parameter $\rho_\omega \sim v/\Delta\omega \sim v\tau_{\text{eff}}$ is connected with the inclusion of uncompleted distant transits.

We note, finally, that, at first sight, there is one further characteristic plasma length, namely, the mean distance between the particles $r_0 \sim N^{-1/3}$. However, this cannot be used as the upper cutoff parameter ρ_m, again because of the long-range character of the perturbation. The point is that, for "weak" interactions with $\rho > \rho_W$, which provide the main contribution to impact broadening [see (2.14)], the situation can be described in terms of perturbation theory in the interaction $\mathbf{d} \cdot \mathbf{F}(t)$ of the dipole moment $\mathbf{d}$ of the atom and the electric field $\mathbf{F}$ of the perturbing particle. The correlation function $K(\tau)$ in second-order perturbation theory is, therefore, expressed in terms of the correlation function $\langle \mathbf{F}(0)\mathbf{F}(\tau)\rangle$ for the electric fields. Kogan has shown[22] that the latter is completely binary, i.e., its dependence on N is trivial: $\langle \mathbf{F}(0)\mathbf{F}(\tau)\rangle \propto N\langle \mathbf{F}_1(0)\mathbf{F}_1(\tau)\rangle$, where $\mathbf{F}_1$ is the single-particle electric field [see (1.4)]. Since the binary correlation function $\langle \mathbf{F}_1(0)\mathbf{F}_1(\tau)\rangle$ does not contain the density, the quantity $N^{-1/3}$ cannot be used as the upper cutoff parameter.

We may now summarize by saying that, if we are to take into account both the Debye shielding and the uncompleted transits, the upper cutoff parameter must be taken to be

$$\rho_m = \frac{\rho_D \rho_\omega}{\sqrt{\rho_D^2 + \rho_\omega^2}}, \tag{2.23}$$

which reduces to the smaller of the two lengths ρ_ω and ρ_D. We recall that we are concerned with the impact region for which $\rho_\omega \gg \rho_W$.

In the static region ($\Delta\omega \gg \Omega$), Eq. (2.21) shows that the line profile is independent of the velocity of the broadening particles. Hence, it is clear that this profile can also be obtained from considerations unrelated to the idea of particle transit. This will be done below (Chap. 3). It is important to note at this point that, in the binary region ($g \ll 1$), the contribution of the individual particles to the line profile is additive, and this is reflected in the fact that $I(\omega)$ is proportional to the particle concentration N.

It is also important to note that the power-law dependence $\gamma(x) \propto x^{-1/2}$ for $x \gg 1$ is valid only in the "positive" static line wing $x > 0$. This wing corresponds to the same signs of the frequency shift $\Delta\omega$ and the Stark constant C. In the negative wing, which is conveniently referred to as the antistatic wing, the intensity falls off in accordance with the exponential law.[17,23,24] [4)]

$$\gamma(x) \propto \exp(-4\sqrt{x}). \tag{2.24}$$

The Stark profile (2.18) is, therefore, asymmetric. Symmetry is conserved only in the impact region $|x| \ll 1$. In the "positive" and "negative" wings, on the other hand, we have power-law and exponential decay, respectively.

The above description of broadening was concerned largely with the binary case ($g \ll 1$). For $g \gg 1$, on the other hand, we must take into account the simultaneous effect of many particles on the chosen atom, and we must consider the question as to how the perturbations of the individual particles are to be added. In the above discussion, we assumed that the energy (frequency) shifts $\varkappa_k$ due to the individual particles can be simply added. At first sight, this seems natural because it corresponds to the addition of the Hamiltonians representing the interaction of the atom with each of the particles. It is clear, however, that, when the Stark shift is evaluated (i.e., each Hamiltonian is diagonalized), we must take a definite coordinate system with the z axis lying along the electric field $\mathbf{F}_k$ producing the given shift $\varkappa_k$. If the number of particles is large, it is not clear

[4)] When the averaging in (2.24) is carried out with the Maxwell distribution function, the exponential decay law is somewhat modified: $\gamma(x) \propto \exp(-x^{3/4})$.

in advance which of the fields $\mathbf{F}_k$ is to be taken parallel to the z axis. The limiting situation is that in which the perturbation is produced by only two charges (say, ions) located at equal distances on either side of the atom.[25] In this case, the resultant shift is $\varkappa = \varkappa_1 + \varkappa_2 = 2\varkappa_1$ although it is clear that the resultant field $\mathbf{F} = \mathbf{F}_1 + \mathbf{F}_2$ acting on the atom is zero.

It follows from the foregoing that the "scalar" addition of the perturbations $\varkappa = \sum_k \varkappa_k$, which corresponds to a new choice of the coordinate system $Oz \parallel \mathbf{F}_k$ in each case, will not, in general, be valid. The only special direction along which the z axis is to be taken is the resultant electric field $\mathbf{F} = \sum_k \mathbf{F}_k$. The resultant shift $\varkappa = (C/e)|\mathbf{F}| = (C/e)|\sum_k \mathbf{F}_k|$ is then determined by the modulus of the vector sum of the fields, and this is not, in general, equal to the sum of the moduli of the individual fields.

It is important to note that this "vector" law of addition for the resultant shift $\varkappa = (C/e)|\sum_k \mathbf{F}_k|$ is independent of the choice of the coordinate system. The system in which the z axis is parallel to $\mathbf{F} = \sum_k \mathbf{F}_k$ is only one of the possible systems, but it is convenient because the evaluation of the shift is then particularly simple. It is possible, however, to select another coordinate system provided its position is fixed in space and is not chosen anew each time, as in the "scalar" model.

The adiabatic theory of broadening based on the vector law of addition of the fields (for arbitrary g) was developed by Kogan.[21] The general expression for the line profile obtained by Kogan[21] is very complicated because of the complicated statistics of the multiparticle plasma microfield (see Chaps. 3 and 4). Apart from the case of the binary static wing, this expression can be simplified only for $g \ll 1$ and $g \gg 1$. In the former case, it yields (2.16), i.e., an expression identical to that obtained for the scalar composition of perturbations. This is readily understood because, when $g \ll 1$, only one particle interacts with the atom and the law of addition is unimportant. For $g \gg 1$, most of the profile is described by the "multiple" static (i.e., Holtsmark; see Chap. 3) profile with corrections for the thermal motion of the perturbing particles corresponding to the adiabatic mechanism of phase modulation (Chap. 4).

We note that the theory of broadening is directly related to the theory of scattering. Thus, in the impact approximation, the line width and shift can be expressed in terms of the cross sections for the scattering of a charged particle by an atom.[26,27] It is easily verified, using (2.17), that the main contribution to the integral in the static result [see (2.18)] is provided by the point t_k defined by the following condition[10]:

$$\varkappa(t_k) = \Delta\omega. \tag{2.25}$$

Condition (2.25) can be looked upon as the condition for the crossing of terms, and the method used to obtain the static result is completely analogous to the Landau–Zener method[15] in the theory of scattering. In the theory of broadening, this result was first used by Jablonski.[28] It was subsequently developed by Szudy,[29] who used the unified quasiclassical approach to obtain the results of both the impact and static theories (see also Szudy and Bailis[30]).

The adiabatic model of broadening has a certain analogy with the model of inelastic transitions in a two-level system during collisions with classical particles. The formula given by (2.17) for the "variable" linewidth $\gamma(\omega)$ has the same structure as the formula for the probability of an inelastic transition obtained by Vaĭnshteĭn *et al.*[31] In the present context, the level separation ω_{12} in the two-level system is replaced by the frequency detuning $\Delta\omega$. The inelastic cross section [or the "variable" linewidth $\gamma(\omega)$] is determined by the Massey parameter $\rho_{eff}\Delta\omega/v$, where ρ_{eff} is the effective impact parameter in the collision (Weisskopf radius in the broadening problem). When $\rho_{eff}\Delta\omega/v \ll 1$, Eq. (2.17) yields, as already noted, the result of the impact theory (2.18), which corresponds (within the framework of perturbation theory) to the Born approximation in the theory of inelastic transitions. When $\rho_{eff}\Delta\omega/v \ll 1$, the transition probability [and linewidth $\gamma(\omega)$] is determined by the existence or otherwise of the term-crossing point (2.25). In the former case, the main contribution to the inelastic transition (and the line profile) is provided by the crossing point, and the transition cross section is given by the Landau–Zener formula [and, correspondingly, the line profile is given by (2.18), i.e., the static theory]. If the crossing point does not exist ("antistatic" wing in broadening), the transition cross section and the line profile exhibit the exponential decay given by (2.24). This analogy enables us to establish similarity relationships between the cross sections for inelastic transitions and the spectral line profiles.[24]

3. THE STATIC HOLTSMARK THEORY. PLASMA MICROFIELD

We shall now consider one of the first treatments of the broadening problem, namely, that formulated by Holtsmark.[1] The essence of this theory is that the electric field produced by ions in the neighborhood of the radiating atom is assumed to be completely static (i.e., the velocity of all the ions is assumed to be zero, and the interaction between the electrons is neglected). Since the ions are distributed randomly in the plasma, each atom "sees" its own ion field F. The emission spectrum corresponding to each Stark component of the atom is, therefore, given by the δ function

$$I_{\alpha\beta}(\omega) = I_{\alpha\beta}\delta(\Delta\omega - C_{\alpha\beta}F) \tag{3.1}$$

with the frequency shifted by the Stark splitting $C_{\alpha\beta}F$.

The observed intensity is obtained by summing the intensities due to the individual atoms or, which amounts to the same thing, by averaging (3.1) over the distribution $W(F)$ of the ion field. The function $W(F)$ determines the probability of each given value of the ion field $\mathbf{F}$ which is the vector sum of the (static) fields $\mathbf{F}_k$ due to the individual particles:

$$\mathbf{F} = \sum_{k=1}^{\mathcal{N}} \mathbf{F}_k = e\sum_{k=1}^{\mathcal{N}} \frac{\mathbf{r}_k}{r_k^3}. \tag{3.2}$$

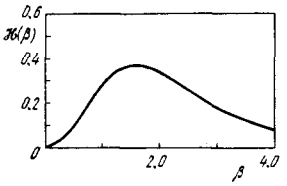

FIG. 2. The Holtsmark distribution $\mathcal{H}(\beta)$.

Integration of (3.1) over all the F with the distribution function $W(F)$ yields the following expression for the static intensity distribution in the $\alpha - \beta$ Stark component:

$$I_{\alpha\beta}(\omega) = \frac{I_{\alpha\beta}}{C_{\alpha\beta}} W\left(\frac{\Delta\omega}{C_{\alpha\beta}}\right). \tag{3.3}$$

The evaluation of the line profile is thus reduced to the determination of the distribution $W(F)$. To evaluate this function, Holtsmark neglected the mutual correlation between the positions of the ions, so that the probability of the configuration $\mathbf{r}_1, \mathbf{r}_1 + d\mathbf{r}_1$; $\mathbf{r}_2, \mathbf{r}_2 + d\mathbf{r}_2$; ...; $\mathbf{r}_N, \mathbf{r}_N + d\mathbf{r}_N$ was proportional to the volume element $d\mathbf{r}_1 d\mathbf{r}_2 \ldots d\mathbf{r}_N (V)^{-N}$ of configuration space.

The probability $W(F)$ is obviously proportional to that part of the configuration space in which (3.2) is satisfied. The required range of the ion coordinates can be automatically isolated by averaging the δ function over all space subject to (3.2):

$$W(\mathbf{F}) = \left\langle \delta\left(\mathbf{F} - \frac{e\sum_{k=1}^{N} \mathbf{r}_k}{r_k^3}\right)\right\rangle = \int d\boldsymbol{\rho}\, e^{i\boldsymbol{\rho}\mathbf{F}} \left\langle \exp\left(\frac{-ie\boldsymbol{\rho}\sum_{k=1}^{N} \mathbf{r}_k}{r_k^3}\right)\right\rangle,$$

where the δ function is expressed in terms of the additional integral with respect to $\boldsymbol{\rho}$. As in the derivation of (2.10), we assume that the particles are independent, and this gives

$$W(F) = \int d\boldsymbol{\rho} e^{i\boldsymbol{\rho}\mathbf{F}} \exp\left[-N\int d\mathbf{r}\,(1 - e^{-ie\boldsymbol{\rho}\mathbf{r}/r^3})\right] = \int d\boldsymbol{\rho} \exp[i\boldsymbol{\rho}\mathbf{F} - N(\lambda e\rho)^{3/2}],$$

where $\lambda = 2\pi(4/15)^{2/3} \approx 2.603$.

Hence, it is clear that the distribution function depends only on the field strength $F = |\mathbf{F}|$. In fact, integrating with respect to the angles defining the direction of the vector ρ, we obtain[32]

$$W(\mathbf{F})\, d\mathbf{F} = W(F) \cdot 4\pi F^2 dF = W(F)\, dF = \mathcal{H}\left(\frac{F}{F_0}\right)\frac{dF}{F}, \tag{3.4}$$

where

$$\mathcal{H}(\beta) = \frac{2}{\pi}\beta \int_0^\infty dx \sin\beta x \exp(-x^{3/2}), \tag{3.5}$$

$$F_0 = \lambda e N^{2/3} \qquad (\lambda \approx 2.603). \tag{3.6}$$

The function $\mathcal{H}(\beta)$ satisfies the normalization condition $\int_0^\infty d\beta\, \mathcal{H}(\beta) = 1$. Figure 2 shows a graph of this function. The maximum value of $\mathcal{H}(\beta)$ corresponds to $\beta = 1.607$. The limiting values are as follows:

$$\mathcal{H}(\beta) \approx \begin{cases} 1.496\beta^{-5/2}(1 + 5.107\beta^{-3/2}), & \beta \gg 1, \\ \frac{4}{3\pi}\beta^2(1 - 0.463\beta^2), & \beta \ll 1. \end{cases} \tag{3.7}$$

The Holtsmark distribution is very different from the Gaussian distribution. It approaches the latter only for small values of β, whereas, for large values of β, it becomes identical with the field distribution due to a single (closest) particle. This is easily understood: small values of β correspond to weak fields due to a large number of ions, and the resultant field, like any sum of a large number of random quantities, may reasonably be expected to follow the Gaussian distribution.[33] As β increases, the ion field begins to be due to a smaller number of particles and, in the limit as $\beta \gg 1$, only one (closest) particle determines the distribution of the (strong) fields. Roughly speaking, therefore, the Holtsmark distribution describes the transition from the Gaussian distribution, corresponding to weak fields, to the binary distribution of strong fields.

We note a useful detail. Although the scale F_0 of the Holtsmark distribution (3.6) should be of the order of magnitude of the average field at the mean interparticle distance, i.e., $F_{av} = e(4\pi N/3)^{2/3} \approx 2.61 eN^{2/3}$, the difference between these two quantities is, in fact, less than 1%.

To obtain the static profile $I_{ab}(\omega)$ of the entire line, we must substitute the Holtsmark distribution (3.4) in (3.3), and then sum over the Stark components α and β of the upper and lower levels and normalize by dividing by the total line intensity $I_0 = \sum_{\alpha,\beta} I_{\alpha\beta}$:

$$I_{ab}(\omega) = \frac{1}{I_0}\sum_{\alpha,\beta}\frac{I_{\alpha\beta}}{C_{\alpha\beta}F_0}\mathcal{H}\left(\frac{\Delta\omega}{C_{\alpha\beta}F_0}\right). \tag{3.8}$$

Line profile calculations based on this expression have been carried out by Underhill and Waddell[34] for a number of hydrogen lines.

It is important to note that the Holtsmark profile is basically nonbinary. According to (3.7), the binary result corresponds only to the line wings, i.e., large values of $\Delta\omega$:

$$I_{ab} \sim \frac{2\pi N}{\Delta\omega^{5/2}}\frac{1}{I_0}\sum_{\alpha,\beta} C_{\alpha\beta}^{3/2} I_{\alpha\beta} \equiv \frac{2\pi N C^{3/2}}{\Delta\omega^{5/2}}, \tag{3.9}$$

where C is the effective Stark constant for the line as a whole. This constant can be estimated from the formula[10,35]

$$C = \left(\frac{3}{8}\right)^{2/3}\frac{h}{m}(n_a^2 - n_b^2) \tag{3.10}$$

where n_a, n_b are the principal quantum numbers of levels a and b.

Both the expression given by (3.9) and the binary result given by (2.21) are linear in the density N of the broadening particles. We note that transition to the binary result occurs for

$$\Delta\omega \gg \frac{C}{e}F_0 = \lambda C N^{2/3} \equiv \Delta\omega_0. \tag{3.11}$$

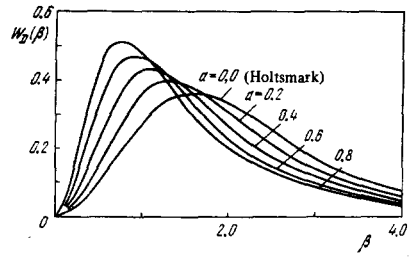

FIG. 3. Electric field distribution $W_D(\beta)$ including ion correlations and Debye screening.

The quantity $\Delta\omega_0$ defines the characteristic scale of the Holtsmark broadening of a hydrogen line. It can easily be estimated from (3.10) and (3.11).

The line profile given by (3.8) satisfies the normalization condition

$$\int_{-\infty}^{\infty} d\omega I_{ab}(\omega) = 1, \tag{3.12}$$

which follows from the normalization of the Holtsmark function.

The Holtsmark theory is thus a departure from the framework of the binary broadening picture. It is based on the "vector" law of addition of the perturbations, and its main restriction is the assumption that the ions are static (this will be discussed in Chap. 4).

The Holtsmark distribution is a simple model of the distribution of the electric microfield produced by ions and electrons in the interior of the plasma. Rigorous evaluation of the distribution function, on the other hand, must take into account the correlation between the ions and the screening of their electric fields by interactions with electrons. The broadening ions in plasma interact with one another through the screened Coulomb potentials

$$V(r_1, r_2, \ldots, r_{\mathcal{N}}) = \sum_{0=k<l}^{\mathcal{N}} \frac{e^2}{r_{kl}} e^{-r_{kl}/\rho_D},$$

where ρ_D is the Debye length.

If the plasma is in thermal equilibrium at temperature T, the probability of a given ion configuration is given by the product of the volume elements $dr_1, dr_2, \ldots, dr_{\mathcal{N}}/(V)^{\mathcal{N}}$ and the additional factor $\exp[-V(r_1 \ldots r_{\mathcal{N}})/kT]$ which represents the interaction between the ions. It is clear that the inclusion of this factor will reduce the probability of configurations with large values of V (i.e., short distances between the ions), which correspond to large values of the fields F. The true distribution function should, therefore, emphasize the probability of weak force fields and reduce the probability of strong fields, as compared with the Holtsmark distribution. The deviation from this distribution depends on the ratio of the mean distance r_0 between the ions $[(4\pi/3)r_0^3 = 1]$ and the Debye length:

$$\alpha = \frac{r_0}{\rho_D} \propto N^{1/6} T^{-1/2}. \tag{3.13}$$

It is clear that α^{-3} is equal to the mean number N_D of particles in the sphere of radius equal to the Debye length. It is also clear that, as $\alpha \to 0$, the distribution function should tend to the Holtsmark distribution. Deviations from the latter increase with increasing α. Figure 3 shows the form of the distribution function for different values of α, as calculated by Hooper.[36] The deviations from the Holtsmark distribution are appreciable only for $\alpha = 4.0$. The number of particles in the Debye sphere is $N_D \approx 16$ in this case.

The criterion for the validity of the Holtsmark theory is

$$\alpha^{-3} = N_D = \frac{4\pi}{3}\left(\frac{kT}{4\pi e^2}\right)^{3/2} N^{-1/2} \gg 1. \tag{3.14}$$

It restricts the applicability of the Holtsmark distribution on the low-temperature side.

We note that there are calculations in the literature[36-39] that, strictly speaking, are valid only when $N_D \gg 1$ for which the deviation from the Holtsmark distribution is small. For $N_D \sim 1$, the accuracy of these calculations is difficult to estimate. A detailed account of effects connected with ion correlations in plasma is given in Kudrin's book.[40]

We must now consider one further generalization of the Holtsmark distribution, which allows for the temporal dynamics of the ion field due to the motion of the particles. The effect of this motion on broadening processes will be considered in Chap. 4. Here, we shall briefly touch upon the behavior of the two-time distribution $W(\mathbf{F}_1, \mathbf{F}_2)$ that determines the probability of observing fields $\mathbf{F}_1$ and $\mathbf{F}_2$ at times $t = 0$ and $t = \tau$, respectively. This problem has been considered by Kogan and Selidovkin.[41]

Calculations of $W(\mathbf{F}_1, \mathbf{F}_2)$ are possible only in the limiting cases of small and large values of τ. As $\tau \to 0$, the result should be the field distribution at two infinitesimally close instants of time for which correlation is fully conserved:

$$W(\mathbf{F}_1, \mathbf{F}_2) = (4\pi F_1^2 F_0)^{-1} \mathcal{H}\left(\frac{F_1}{F_0}\right) \delta(\mathbf{F}_1 - \mathbf{F}_2). \tag{3.15}$$

The characteristic time τ_p for the violation of correlation can be determined from the condition that the average (for given F_1) change in the field $\Delta F^2 = \langle |\mathbf{F}_1 - \mathbf{F}_2|^2 \rangle$ during the time τ_p should be of the same order as F_1 itself, i.e., $\langle \Delta F^2 \rangle \approx F_1^2$. This gives

$$\tau_p \approx (N^{1/3} v_0)^{-1} \begin{cases} 4.4\beta_1, & \beta_1 \ll 1, \\ 15\beta_1^{-1/2}, & \beta_1 \gg 1, \end{cases} \tag{3.16}$$

where $v_0 = \sqrt{2kT/M}$ is the ion velocity and $\beta_1 = F_1/F_0$.

It is clear from (3.16) that correlation is most rapidly lost by small ($\beta_1 \ll 1$) and large ($\beta_1 \gg 1$) fields. These estimates agree with estimates of the mean field lifetime (Chap. 4).

For large values of τ, the distribution function is $[P(\beta) = \mathcal{H}(\beta)/4\pi\beta^2]$:

$$W(\beta_1, \beta_2) = P(\beta_1) P(\beta_2) + \frac{8\sqrt{\pi} P'(\beta_1) P'(\beta_2)}{3\lambda^2 N^{1/3} v_0 \tau} \frac{(\beta_1\beta_2)}{\beta_1\beta_2}. \quad (3.17)$$

The leading term in (3.17) is, as expected, the product of the two independent Holtsmark solutions. The second term describes the slowly ($\propto 1/\tau$) decaying field correlation. By comparing the second term in (3.17) with the first, we can estimate the characteristic time necessary to "induce correlation":

$$\tau_i \approx (N^{1/3} v_0)^{-1} \times \begin{cases} 0.8, & \beta_1, \beta_2 \ll 1, \\ 14\beta_1^{-1}\beta_2^{-1}, & \beta_1, \beta_2 \gg 1. \end{cases} \quad (3.18)$$

Hence, it is clear that correlation is more rapidly induced for high fields ($\beta_1, \beta 2 \gg 1$) than for low fields.

4. EFFECT OF THE THERMAL MOTION OF IONS

The fact that the broadening problem can be treated on the basis of the static plasma field distribution function is hardly obvious in advance.[5)] In fact, the very existence of plasma is connected with sufficiently high temperatures at which ions have considerable velocities. This means that the ion field varies with time, and it is important to establish the conditions under which this variation may be neglected. The most direct method is to calculate the corrections to the static line profile due to the thermal motion of the ions. The criterion for the ions to be static is then equivalent to the requirement that these corrections must be small in comparison with the zero-order (static) approximation. Holstein[43] has carried out this program in the binary case. For the multiple (Holtsmark) broadening, the "thermal" corrections were first calculated by Kogan[21] within the framework of the phase modulation model. Wimmel[44] used the same model to give a clear physical picture of the effect of the thermal motion of the ions on the atom. A complete calculation of thermal corrections, including nonadiabatic effects, has been carried out by Sholin *et al.*[45]

We shall consider, to begin with and following Wimmel,[44] the general properties of the thermal motion effects within the framework of the phase modulation model.

Suppose that the ion field $F(t)$ varies sufficiently slowly, so that the correlation function (2.3) can be expanded into a series in powers of the field derivatives $\dot{F}$. If we then substitute (2.3) in (1.1), we obtain

$$I_{ab}(\omega) \approx \int_0^\infty dF W(F) \frac{1}{\pi} \operatorname{Re} \int_0^\infty d\tau e^{-i[\Delta\omega - (CF/e)]\tau} \langle e^{i(C\dot{F}\tau^2/2e)} \rangle_F, \quad (4.1)$$

where we have confined our attention to the first derivative of the field $\dot{F}$ and have divided the averaging process into two stages: we first average over all the $\dot{F}$ for a fixed field F (this is indicated by $\langle \ldots \rangle_F$) and then over all the fields F with the Holtsmark distribution function $W(F)$.

The inner integral with respect to τ in (4.1) is the spectrum of the atom for a fixed field F and, in the absence of the thermal motion ($\dot{F} \equiv 0$), gives the δ function of (3.1). The factor within $\langle \ldots \rangle_F$ obviously describes the loss of phase coherence by the atom as a result of the thermal motion of the ions. In fact, when $|C\dot{F}\tau^2/2e| \sim 1$, the atom "forgets" its original phase, and this leads to the spreading of the spectrum for given F by the amount $|C\dot{F}/e|^{-1/2}$. The time T_{ph} during which phase coherence is lost is given by the following order-of-magnitude formula:

$$T_{ph}(F) \sim \left\langle \left| \frac{C}{e} \dot{F} \right|^{-1/2} \right\rangle_F \sim \sqrt{\frac{T_F e}{CF}}, \quad (4.2)$$

where $T_F \sim F\langle |\dot{F}|^2 \rangle_F^{-1/2}$ is the mean lifetime of the field F.

The loss-of-coherence time T_{ph} is thus related to the finite magnitude of the ion field lifetime T_F. To calculate the latter, we must know the field derivatives $\langle \dot{F}^2 \rangle_F$ for given F. Such calculations have been carried out by Chandrasekhar and von Neumann.[32] We shall be interested in the components $\langle \dot{F}_\parallel^2 \rangle_F$ and $\langle \dot{F}_\perp^2 \rangle_F$, respectively parallel and perpendicular to the field vector **F**:

$$\langle \dot{F}_\parallel^2 \rangle_F = \frac{45}{8} (\omega_F F_0)^2 \times \begin{cases} 1.3, & \beta \ll 1, \\ 16\beta^3.45, & \beta \gg 1. \end{cases} \quad (4.3)$$

$$\langle \dot{F}_\perp^2 \rangle_F = \frac{45}{8} (\omega_F F_0)^2 \times \begin{cases} 2.3, & \beta \ll 1, \\ 8\beta^3.45, & \beta \gg 1. \end{cases} \quad (4.4)$$

where $\omega_F = \lambda^{1/2} v_0 N^{1/3} (\lambda \approx 2.603)$ is the characteristic scale of the field frequency and $\beta = F/F_0$. The derivatives given by (4.3) and (4.4) for any β differ from one another only by numerical factors of the order of unity. It is, therefore, unimportant as to which of them is used to determine T_F. Using (4.3) and (4.4), we obtain

$$T_F \sim F(|\dot{F}|^2)_F^{-1/2} \sim (N^{1/3} v_0)^{-1} \begin{cases} \beta, & \beta \ll 1, \\ \beta^{-1/2}, & \beta \gg 1, \end{cases} \quad (4.5)$$

i.e., intermediate fields ($\beta \sim 1$) have the maximum lifetime, whereas weak ($\beta \ll 1$) and strong ($\beta \gg 1$) fields have short lifetimes.

Equations (4.2) and (4.5) can be used to formulate the static criterion. Thus, the field F can be regarded as static if the atom loses coherence before the ion field succeeds in changing, i.e.,

$$T_{ph} \ll T_F, \quad \text{or} \quad \frac{C}{e} F T_F |_{CF/e = \Delta\omega} \gg 1. \quad (4.6)$$

Let us consider what happens to the criterion given by (4.6) for large and small values of $\Delta\omega(CF/e)$. From (4.5) and (4.6) we have

$$\Delta\omega \gg \begin{cases} \frac{v^2}{C} \equiv \Omega, & \Delta\omega \gg \Delta\omega_0, \quad (4.7a) \\ \sqrt{CNv}, & \Delta\omega \ll \Delta\omega_0. \quad (4.7b) \end{cases}$$

When these conditions are analyzed, it is important to bear in mind the value of the parameter $g_i = N(C/v_i)^3$.

[5)] Thus, in 1926, Pauli wrote:[42] "Holtsmark undertook to interpret pressure broadening of a spectral line in terms of the Stark effect produced by intermolecular fields. Holtsmark's results are not altogether well founded because the intermolecular fields that he introduced cannot be regarded as uniform or, still less, time-independent." (The author is indebted to G. V. Sholin and A. V. Demura for bringing this quotation to his attention.)

When $g_i \ll 1$ (binary region), the static approximation is valid only in the distant wing for which $\Delta\omega \gg \Omega \gg \Delta\omega_0$. When $g \gg 1$ (multiple case), the static theory is valid throughout, with the exception of the central part of the profile, where $\Delta\omega_0 \gg \Delta\omega \gg \sqrt{CNv_i}$. The validity of the Holtsmark approximation is thus found to improve as the parameter g increases and as we move further outward in the line wing.

Let us now proceed to a quantitative calculation of the thermal corrections to the static line profile. So far, our discussion has been based on the assumption that the ion field $\mathbf{F}(t)$ varies only in magnitude (modulus). This variation is clearly connected with the derivatives $\dot{\mathbf{F}}_\parallel$ that are parallel to the field. In reality, the true ion field $\mathbf{F}(t)$ will also vary in direction. This is due to the derivative $\dot{\mathbf{F}}_\perp$ and leads to two important effects. If the rotation of the vector $\mathbf{F}(t)$ occurs sufficiently slowly, the dipole moment $\mathbf{d}$ of the atom can follow this variation adiabatically, and its component along the direction of $\mathbf{F}$ remains constant. With this type of reorientation of the atom, the component of $\mathbf{d}$ along the direction of propagation of the light wave, $\mathbf{k}$, will vary, and since the square of this component determines the intensity of the radiation emitted by the atom, we should have a certain *amplitude* modulation.

In addition to the amplitude modulation, rotation of the quantization axis is accompanied by nonadiabatic effects connected with the fact that the atom lags behind the field $\mathbf{F}(t)$. Thus, if we direct one axis of a rotating system of coordinates along the field $\mathbf{F}$, we shall have in this system an additional interaction between the orbital angular momentum of the system $\mathbf{L}$ and the "magnetic" field. This interaction leads to a change in the wave function and in the energy of the radiating atom which will, of course, affect the corresponding matrix elements of the dipole moment and the phase of the radiated wave.

Let the x axis of the rotating system of coordinates lie along the vector $\mathbf{F}(t)$. We now transform the wave function ψ to this rotating system:

$$\psi' = e^{iL_z\varphi(t)/\hbar}\psi, \tag{4.8}$$

where ψ' is the wave function in the rotating system, L is the orbital angular momentum of the atom, and $\varphi(t)$ is the angle through which the field $\mathbf{F}$ rotates in a time $t[\varphi(0)=0]$. Substituting (4.18) in the Schrödinger equation, we obtain the equation for the function ψ':

$$i\hbar\frac{\partial\psi'}{\partial t} = [\hat{\mathcal{H}}_0 - d_x F(t) + L_z\dot{\varphi}(t)]\psi', \tag{4.9}$$

where $\hat{\mathcal{H}}_0$ is the unperturbed Hamiltonian for the atom.

It is clear that, in the rotating system, we have both the electrostatic ($d_x F$) and "magnetic" ($L_z\dot{\varphi}$) perturbation. The latter is connected with the instantaneous angular velocity $\dot{\varphi}$ of the field. The appearance of this perturbation is, obviously, a consequence of the Larmor theorem.[46] Our aim is to develop a perturbation theory in the rate of change of the field $\dot{F}$. The derivative of the modulus of the field $\dot{F}$ is related to $\dot{\mathbf{F}}_\parallel$, whereas the angular velocity $\dot{\varphi}(0)$ is given by

$$|\dot{\varphi}(0)| = \left|\frac{\mathbf{F}(0)\dot{\mathbf{F}}(0)}{F^2}\right| = \left|\frac{\dot{\mathbf{F}}_\perp}{F}\right|. \tag{4.10}$$

Solution of (4.9) by perturbation theory methods can be used to express the corrections for the thermal motion of the ions in terms of the mean squares of the field derivatives given by (4.2) and (4.4). For the center of the line (small values of $\Delta\omega$ and $F \to 0$), these corrections are found to increase rapidly as a result of the nonadiabatic effects. Thus, it is clear from (4.9) that the nonadiabatic corrections to the wave function ψ due to rotation are determined by the ratio $\dot{\varphi}/d_x F$ or, according to (4.10), by the ratio $|\dot{\mathbf{F}}_\perp|/F^2$ which increases rapidly as $F \to 0$.

When the thermal motion of the ions is taken into account, the hydrogen line profile $I(\omega)$ can be written as the sum of two terms, namely, the zeroth term $I^{(0)}$ (Holtsmark term) and the correction term $I^{(1)}$ describing the effects associated with thermal motion:

$$I(\omega) = I^{(0)}(\omega) + I^{(1)}(\omega) = \frac{1}{\Delta\omega_0}\left[\mathcal{H}\left(\frac{\Delta\omega}{\Delta\omega_0}\right) + g^{-2/3}\Pi\left(\frac{\Delta\omega}{\Delta\omega_0}\right)\right], \tag{4.11}$$

$$\Pi(x) \approx \begin{cases} a_1 x^{-7/2}, & x \gg 1, \\ a_2 x^{-2}, & x \ll 1, \end{cases} \tag{4.12}$$

where a_1, a_2 are numerical constants that depend on the particular line under investigation.

The thermal correction $I^{(1)}$ is proportional to the ion temperature T (it enters through the factor $g^{-2/3} \propto v_0^2 \propto T$) and contains the function $\Pi(x)$ which describes phase and amplitude modulation and nonadiabatic effects.

In the line wing ($x \gg 1$), the thermal correction is $\Pi(x) \propto x^{-7/2}$, i.e., it decreases more rapidly than the Holtsmark function in such a way that the contributions of all three effects to the correction are of the same order. At the line center ($x \ll 1$), there is a rapid increase in the thermal correction [$\Pi(x) \propto x^{-2}$]. This effect is wholly due to the fact that the rotation is nonadiabatic, whilst the phase and amplitude modulation effects tend to a constant and are, therefore, relatively small. These results are valid for any hydrogen line.

The condition for the validity of the static Holtsmark theory is, obviously, the requirement that the second term in (4.11) be small in comparison with the first. It can be shown that this is equivalent to the criteria given by (4.6) and (4.7) above. It is now clear, however, that, in contrast to the Holtsmark approximation itself, deviations from this approximation are due to nonadiabatic effects, i.e., the fact that the adiabatic oscillator model is no longer valid. In terms of the criterion given by (4.6), we may say that the main reason for the loss of coherence by the atom is not phase modulation but the presence of nonadiabatic transitions between Stark components due to the rotation of the ion field.

To summarize, we note that the Holtsmark theory has a definite range of validity. Effects associated with ion-ion correlation restrict the validity of this theory on the side of low temperatures [condition (3.14)], whereas thermal-motion effects restrict it on the high-

temperature side (the condition $g = N(C/v)^3 \gg 1$). If we compare these conditions, we see that the width of the region in which the Holtsmark theory is valid is defined by

$$\frac{n^2}{4\pi}\frac{M}{m}\frac{n^2-a_0}{N^{-1/3}} \gg 1, \tag{4.13}$$

where n is the principal quantum number of the broadened level, M, m are the ion and electron masses, and a_0 is the first Bohr radius. The condition $n^2 a_0/N^{-1/3} \ll 1$ obviously defines the degree of inhomogeneity of the ion field within the region occupied by the atom (see Chap. 10 for further details). The inequality given by (4.13) is equivalent to $N \gg 10^{14}$ cm^{-3} for initial hydrogen lines corresponding to $n = 3, 4, 5$.

5. IMPACT APPROXIMATION. HYDROGEN LINE PROFILE FOR A FIXED ION FIELD

We shall now consider the impact approximation which is valid for broadening by fast particles (usually electrons). For such particles, $g_e = N(C/v_e)^3 \ll 1$ and most of the line profile lies in the impact region. It is only in the distant wings, where $\Delta\omega \gtrsim \Omega_e$, that transition from the impact to the static broadening mechanism is possible.

The theory of impact broadening for hydrogen levels must, from the very outset, take into account nonadiabatic transitions between degenerate states corresponding to the same level with a given principal quantum number n. It is important to note, however, that degeneracy of the hydrogen levels in plasma is removed by the presence of the statistical ion field F_i. All calculations on impact broadening by electrons must, therefore, be carried out in the parabolic coordinates with the z axis parallel to F_i, so that the interaction between the atom and the ion field is diagonal.

The modern theory of impact broadening was developed in the papers of Sobel'man,[26] Griem *et al.*,[47] and Vaĭnshteĭn and Sobel'man.[48] Our account will follow the expositions given by Griem *et al.*,[49] Deutsch *et al.*,[50] and Sholin *et al.*[51]

The wave function $\psi(t)$ of both levels satisfies the Schrödinger equation

$$i\hbar\frac{\partial\psi}{\partial t} = [\hat{\mathcal{H}}_0(F_i) + \hat{V}_e(t)]\,\psi, \tag{5.1}$$

where the zero-order Hamiltonian $\hat{\mathcal{H}}_0$ includes the interaction with the ion field F_i and $\hat{V}_e(t) = -\mathbf{d}\cdot\mathbf{F}_e(t)$ represents the interaction between the dipole moment $\mathbf{d}$ of the atom and the electron field $\mathbf{F}_e(t)$ [see (1.4)].

It is convenient to introduce the evolution operator $U(t, 0)$ in the interaction representation:

$$\psi(t) = e^{-i\hat{\mathcal{H}}_0(F_i)t/\hbar}\hat{U}(t, 0)\,\psi(0). \tag{5.2}$$

The operator $\hat{U}$ satisfies the equation

$$i\hbar\frac{\partial\hat{U}}{\partial t} = e^{i\hat{\mathcal{H}}_0 t}\hat{V}_e(t)\,e^{-i\hat{\mathcal{H}}_0 t}\hat{U} = \hat{\tilde{V}}_e(t)\,\hat{U}, \tag{5.3}$$

whose formal solution is

$$\hat{U}(t, 0) = \tilde{T}\exp\left[-\frac{i}{\hbar}\int_0^t \hat{\tilde{V}}_e(\tau)\,d\tau\right] \tag{5.4}$$

where $\tilde{T}$ is the chronological order operator.

The line profile of (1.1) and (1.2) can easily be written down with the aid of the evolution operators $\hat{U}_a$ and $\hat{U}_b$ for both levels:

$$I_{ab}(\omega) = \mathrm{Re}\sum_{\substack{\alpha,\alpha',\sigma\\ \beta,\beta'}}\int_0^\infty dt e^{i(\omega-\omega_{\alpha\beta})t}\langle\beta\,|\,d_\sigma\,|\,\alpha\rangle \times\langle\alpha'\,|\,d_\sigma\,|\,\beta'\rangle\{\langle\alpha\,|\,\hat{U}_a(t, 0)\,|\,\alpha'\rangle\langle\beta\,|\,\hat{U}_b^*(t, 0)\,|\,\beta'\rangle\}, \tag{5.5}$$

where d_σ is the dipole moment component and the symbol $\{\ldots\}$ represents averaging over the coordinates and velocities of the perturbing electrons. It will be convenient to use the notation

$$\langle\alpha\,|\,U_a\,|\,\alpha'\rangle\langle\beta\,|\,U_b^*\,|\,\beta'\rangle = \langle\langle\alpha\beta\,|\,U_a U_b^*\,|\,\alpha'\beta'\rangle\rangle.$$

We shall now try to simplify the expressions for U_a and U_b corresponding to (5.4) [and hence for the spectrum $I_{ab}(\omega)$] by using the impact approximation. This can be done if we are interested in time intervals Δt that are large in comparison with the collision time ρ/v. At the same time, the interval Δt must be small in comparison with the time γ^{-1} between collisions (γ is the impact width due to collisions), so that the increase in the operator U in the interval Δt is still small. All this is equivalent to

$$\rho/v \ll \Delta t \ll \gamma^{-1}.$$

Assuming $\gamma \sim Nv\pi\rho^2$, we see that the condition for the existence of this kind of region is that the collisions must be binary: $N\rho^3 \ll 1$.

Consider the change in the operator product $U_a U_b^*$ during the time Δt:

$$\Delta U_a(t, 0)\,U_b^*(t, 0) = U_a(t+\Delta t, 0)\,U_b^*(t+\Delta t, 0) - U_a(t, 0)\,U_b^*(t, 0) = [U_a(t+\Delta t, t)\,U_b^*(t+\Delta t, t) - 1]\,U_a(t, 0)\,U_b^*(t, 0). \tag{5.6}$$

We must now average (5.6) over the collision parameters. Since $\Delta t \gg \rho/v$, the increase in the operators $U_a U_b^*$ on the interval $(t, t+\Delta t)$ is independent of the quantity $U_a(t, 0)U_b^*(t, 0)$, and averaging of the two cofactors on the right-hand side of (5.6) can be carried out separately. The average product $\{U_a U_b^*\}$ is then the solution of

$$\frac{\Delta\{U_a(t, 0)\,U_b^*(t, 0)\}}{\Delta t} = e^{i(\hat{\mathcal{H}}_{0a}-\hat{\mathcal{H}}_{0b})t}\hat{\Phi}_{ab}e^{-i(\hat{\mathcal{H}}_{0a}-\hat{\mathcal{H}}_{0b})t}\{U_a(t, 0)\,U_b^*(t, 0)\}, \tag{5.7}$$

where the time-independent operator Φ_{ab} is called the electron impact broadening operator and is given by

$$\hat{\Phi}_{ab} = \frac{1}{\Delta t}\{\hat{U}_a(t, t+\Delta t)\,\hat{U}_b^*(t, t-\Delta t) - 1\}. \tag{5.8}$$

The solution of (5.7) can be written in the form

$$\{U_a U_b^*\} = e^{i(\mathcal{H}_{0b}-\mathcal{H}_{0a})t/\hbar} e^{\{-i[(\mathcal{H}_{0a}-\mathcal{H}_{0b})/\hbar]+\hat{\Phi}_{ab}\}t}. \quad (5.9)$$

Substituting (5.9) in the expression for the spectrum given by (5.5), we obtain the line profile in the impact approximation:

$$I_{ab}(\omega) = -\mathrm{Re} \sum_{\alpha,\alpha';\beta,\beta';\sigma} \langle\beta | d_\sigma | \alpha\rangle \langle\alpha' | d_\sigma | \beta'\rangle \times \langle\langle\alpha\beta | \left[i\omega - \frac{i}{\hbar}(\mathcal{H}_{0a} - \mathcal{H}_{0b}) - \Phi_{ab} \right]^{-1} | \alpha'\beta'\rangle\rangle. \quad (5.10)$$

Thus, the precise determination of the evolution operator $\hat{U}(t,0)$ and the line profile $I_{ab}(\omega)$ reduces in the impact approximation to the determination of the simpler electron impact broadening operator Φ_{ab}.

Since $\Delta t \gg \rho/v$, the evolution operator in (5.8) can be replaced on the interval $(t, t+\Delta t)$ by the scattering matrixes S_a and S_b. We then have

$$\Phi_{ab} = N \int_0^\infty dv v f(v) \int_0^\infty 2\pi\rho\, d\rho \{S_a S_b^* - 1\}. \quad (5.11)$$

where the symbol $\{\ldots\}$ represents averaging over the position angles of the vectors $\boldsymbol{\rho}$ and $\mathbf{v}$, and $f(v)$ is the Maxwell electron velocity distribution.

The evaluation of the operator Φ_{ab} involves the determination of the scattering matrix S, and this is still a very complex problem. It can, however, be simplified by using the fact that, when the S matrix is evaluated, it turns out that the perturbation theory in $\tilde{V}(t)$ is valid [see (5.3)]. This is connected with the long-range character of the Coulomb field. In fact, the structure of (5.11) is completely analogous to that of (2.14) in the adiabatic theory of broadening, and the analog of the S matrix is the quantity $\cos\int_{-\infty}^{\infty} \varkappa(t)dt = \cos(\pi C/\rho v)$. When (2.14) was analyzed, we saw that the main contribution to broadening was provided by distant (weak) transits with $\rho > \rho_W$ for which perturbation theory can be used.

Precisely the same considerations enable us to replace the exact S matrix in (5.11) by its expansion into a perturbation-theory series up to the second order.

We recall that evaluation of the S matrix by perturbation theory is only logarithmically precise, and the accuracy is usually no better than 20–30%. To improve the accuracy, the logarithmic term is augmented by the term representing the contribution of strong collisions with $\rho < \rho_W$. The latter collisions are taken into account on the basis of approximate formulas (for example, those of the adiabatic model) which, nevertheless, give results that are close to one another.[52]

Let us begin by considering the broadening of level a, for which the S matrix in second-order perturbation theory is of the form

$$\{S_a - 1\} = \left\{ -\frac{i}{\hbar}\int_{-\infty}^{\infty} \tilde{V}_a(t)\,dt + \left(-\frac{i}{\hbar}\right)^2 \int_{-\infty}^{\infty} dt_1 \tilde{V}_a(t_1) \int_{-\infty}^{t_1} dt_2 \tilde{V}_a(t_2) \right\}. \quad (5.12)$$

The next step is to substitute the explicit expression for the perturbation $\tilde{V}_a(t) = e^{-i\mathcal{H}_0 t} e\mathbf{r}_a \cdot \mathbf{F}(t) e^{i\mathcal{H}_0 t}$ and to perform the averaging over the position angles of the vectors $\boldsymbol{\rho}$ and $\mathbf{v}$ in $\mathbf{F}(t)$. The first term on the right-hand side of (5.12) is then found to vanish and, after a number of transformations and substitution in (5.11), the second term gives[47,49–51]

$$\Phi_a = \frac{16}{3} N \frac{e^4}{\hbar^2} \langle v\rangle^{-1} \mathbf{r}_a \mathbf{r}_a \Lambda, \quad \Lambda \equiv \ln \frac{\rho_m}{\rho_W(v_0)} + 0.215, \quad (5.13)$$

where the numerical coefficient in front of the logarithm represents the contribution of strong collisions and $v_0 = \sqrt{2kT/m}$.

The formula given by (5.13) is a generalization of the adiabatic result given by (2.13) and (2.14). In particular, the square of the Stark constant in (2.14) is replaced in (5.13) by the operator $(e^4/\hbar^2)\mathbf{r}_a\mathbf{r}_a$. The upper cutoff parameter ρ_m must, according to Chap. 2, be set equal to the smaller of the two values ρ_D and $\rho_\omega = v/\Delta\omega$ [see (2.23)]. We note that the splitting of the levels in the ion field $CF/e \sim CN^{2/3}$ does not appear in the final result for the operator Φ_a. This is so because the magnitude of this splitting $CN^{2/3}$ is small in comparison with the reciprocal collision time between the electron and the atom $\tau^{-1} \sim v_e/\rho_{eW} \sim v_e^2/C \sim \Omega_e$.

Generalization of (5.13) to the case of broadening of both levels presents no difficulty. The operator Φ_{ab} then contains both the second-order perturbation-theory terms $\mathbf{r}_a\mathbf{r}_a$ and $\mathbf{r}_a\mathbf{r}_b^*$ and the cross term involving the products of first-order terms:

$$\Phi_{ab} = -\frac{16}{3} N \frac{e^4}{\hbar^2} \langle v\rangle^{-1} (\mathbf{r}_a\mathbf{r}_a - \mathbf{r}_a^*\mathbf{r}_b^* - 2\mathbf{r}_a\mathbf{r}_b^*) \Lambda. \quad (5.14)$$

Hence, it is clear that the contributions of the upper and lower levels to impact broadening are not additive.

As already noted, the evaluation of the matrix elements of the operators Φ_{ab} must be carried out in the parabolic system of coordinates with the z axis lying along the ion field. For the matrix elements of the operators $\mathbf{r}\cdot\mathbf{r}$, this yields[51]

$$\langle n_1 n_2 m | \mathbf{r}\cdot\mathbf{r} | n_1 n_2 m\rangle = a_0^2 \frac{9}{4} n^2 [n^2 + (n_1 - n_2)^2 - m^2 - 1], \quad (5.15)$$

$$\left.\begin{aligned} \langle n_1 - 1, n_2 + 1, m | \mathbf{r}\cdot\mathbf{r} | n_1 n_2 m\rangle &= a_0^2 \frac{9}{4} n^2 \sqrt{n_1 (n - n_1)(n_2 + 1)(n - n_2 - 1)}, \\ \langle n_1 + 1, n_2 - 1, m | \mathbf{r}\cdot\mathbf{r} | n_1 n_2 m\rangle &= a_0^2 \frac{9}{4} n^2 \sqrt{n_2 (n - n_2)(n_1 + 1)(n - n_1 - 1)}. \end{aligned}\right| \quad (5.16)$$

The operator Φ_{ab} must now be substituted into the general formula (5.10) for the line profile $I_{ab}(\omega)$. Calculations of this profile involve laborious numerical procedures for the diagonalization of the resolvent operator $[i\omega - i(\hat{\mathcal{H}}_{0a} - \hat{\mathcal{H}}_{0b})/\hbar + \hat{\Phi}_{ab}]^{-1}$, and the complexity of this increases with the number of components in the line. For the approximate determination of the impact linewidth γ, we can neglect nondiagonal matrix elements of Φ_{ab} and sum the diagonal elements with weights equal to the component intensities[6]:

$$\gamma = \sum_{\alpha,\beta} |d_{\alpha\beta}|^2 \frac{\langle\langle\alpha\alpha | \Phi_{ab} | \beta\beta\rangle\rangle}{\sum_{\alpha,\beta} |d_{\alpha\beta}|^2}. \quad (5.17)$$

[6] We note that the formula given by (5.17) is exact for the line wing.

For rough estimates, we can use the expression

$$\gamma = \frac{16}{3} N \frac{e^4}{\hbar^2} \sqrt{\frac{\pi m}{8kT}} (n_a^4 - n_b^4) \left(\ln \frac{\rho_{max}}{\rho_W(v_0)} + 0.215 \right). \qquad (5.18)$$

We note that this formula is only valid for the lower lines. For transitions with quantum numbers $n_a \gg 1$, $n_b \gg 1$, $|n_a - n_b| \ll n_a$, the cross term in (5.14) leads to strong compensation of the width of the individual levels, and this may give a weaker dependence on n, namely, $\gamma \propto n^2$.[53]

The resulting picture of electron impact broadening in the ion field can be described schematically as follows. The ion field splits the hydrogen line into the individual Stark components which are broadened by electron impacts. The impact widths of these components are determined by the diagonal matrix elements (5.14) of the operator Φ_{ab}.

The line profile broadened by electrons in a fixed ion field has a very complicated structure. As noted above, its evaluation involves the diagonalization of the resolvent operator in (5.10). This can be done analytically only for the simplest lines ($Ly-\alpha$, $Ly-\beta$), and was first carried out by Strekalov and Burshtein,[54] and by Pfennig.[55] We shall follow Sholin *et al.*[51]

Consider the eigenvalues E_α and eigenfunctions $|\psi_\alpha\rangle$ of the Hamiltonian $\hat{\mathcal{H}}_0(F)/\hbar - i\hat{\Phi}_a$, which includes the interaction with the ion field F and electron impact broadening $\hat{\Phi}_a$. The eigenfunctions $|\varphi_\beta\rangle$ of the Hamiltonian $\hat{\mathcal{H}}_0(F)$ are known. We can, therefore, find the matrix $C_{\beta\alpha}$ defining the transformation from the basis $|\varphi_\beta\rangle$ to the basis $|\psi_\alpha\rangle$. The operator $H_0 - i\Phi$ is not Hermitian and, therefore, the system of ket vectors $|\psi_\alpha\rangle$ must be augmented by the orthogonal system of bra vectors $\langle\chi_\alpha|$. This system is obtained from $\langle\varphi_\beta|$ with the aid of the matrix $C^{-1}_{\alpha\beta}$. Since the operator $\hat{\mathcal{H}}_0 - i\Phi$ is not Hermitian, the matrix $\hat{C}$ is not unitary: $C^{-1} \neq C^+$. Having found the functions $|\psi_\alpha\rangle$ and $\langle\chi_\alpha|$, we must obviously diagonalize the resolvent operator and then obtain the line profile. The problem is thus reduced to the determination of the matrix $\hat{C}$. Consider the simplest hydrogen line $Ly-\alpha$. The operator Φ_a for this line has only one nondiagonal matrix element connecting the symmetric lateral components. The energy eigenvalues are

$$E_{1,2} = \omega \pm \Omega - iw, \quad \Omega \equiv \sqrt{\left(\frac{\Delta}{2}\right)^2 - \beta^2}; \qquad (5.19)$$

where w and β are, respectively, the diagonal and nondiagonal matrix elements of Φ_a, and Δ is the level splitting in the ion field. It is clear from (5.19) that the presence of the non-Hermitian nondiagonal element leads to a peculiar effect, namely, the energy levels E_1 and E_2 do not repel because of the presence of β but, on the contrary, are found effectively to attract. In particular, when $\beta = \Delta/2$, we have the point $E_1 = E_2$ at which the two states degenerate (collapse). The character of the spectrum undergoes a substantial change at this point because the quantity Ω becomes purely imaginary for $\Delta/2 < \beta$. The contribution of the lateral components to the line intensity outside the collapse region has the form[54]

$$I(\omega) = \frac{|d_{10}|^2}{\pi} \left[\frac{w + (\beta/\Omega)(\Delta\omega + \Omega)}{(\Delta\omega + \Omega)^2 + w^2} + \frac{w - (\beta/\Omega)(\Delta\omega - \Omega)}{(\Delta\omega - \Omega)^2 + w^2} \right]. \qquad (5.20)$$

The contribution of the nondiagonal matrix element β is important near the line center at which $\Delta\omega = 0$ but, in the wings, it plays only a minor role. In the collapse region $\Delta/2 < \beta$ and the character of the spectrum is found to change. Here, the quantity Ω is additive to the diagonal matrix element w, and the collapse effect leads to a certain narrowing of the line. At the same time, it must be recalled that the collapse effect occurs only for weak ion fields F for which the splitting Δ is comparable with the impact half-width of the line $w \sim \beta$ and the statistical weight is small. Nevertheless, collapse may be important for the line shape at the line center.

For lines containing a large number of components (for example, for lines in the Balmer series), analytic diagonalization of the resolvent is very difficult. Usually, the inversion of the matrices in the spectrum given by (5.10) is carried out numerically on a computer (see Chap. 10).

6. EXACT SOLUTION OF THE BROADENING PROBLEM IN THE BINARY APPROXIMATION

The specific properties associated with the additional degeneracy in a Coulomb field can be used to obtain an exact solution for the hydrogen-line broadening in the case of binary collisions with charged particles (usually electrons). This is connected with the fact that it is possible to find the exact wave functions of the excited state of hydrogen in the field of the incident charged particle. The history of this problem is of some interest. This solution was first obtained by Spitzer[56] as far back as 1940 for the special case of the $Ly-\alpha$ line. For over thirty years, this result did not produce its due response in the theory of broadening. Exact wave functions for the $n = 2$ level were then independently obtained by Chibisov,[57] who used them for scattering problems.[7] It is only recently that Spitzer's results were resurrected by Pfennig,[59] who used them to investigate the transition between the static and impact limits of the theory of broadening. At virtually the same time, Lisitsa and Sholin[60] put forward a method for finding the exact wave functions corresponding to any hydrogen level in the electric field of an incident charge. In this method, the collision problem is reduced to the problem of energy levels and wave functions of the hydrogen atom in crossed electric and magnetic fields. The latter problem was formulated in the 1920's[61] and its solution (in the case of static fields) was given by Demkov *et al.*,[62] who used the additional (four-dimensional) symmetry of the hydrogen atom to avoid the laborious solution of the secular equations in the traditional approach. These methods were subsequently used to solve a number of problems in the theory of scattering.[63,64]

To elucidate the essence of the method let us begin by

---

[7] The interaction of charged particles with the hydrogen atom in the $n = 2$ state was also considered by Seaton[58] in connection with scattering problems.

a model example,[8] namely, the emission spectrum of a hydrogen atom in a rotating electric field.[65,66]

Consider an excited hydrogen atom in an electric field **F** which rotates about the z axis in the x, y plane with angular velocity Ω.[9] We shall suppose that the modulus of the electric field remains constant. We now introduce a rotating coordinate system x', y', z' ($z'=z$), the x' axis of which is always parallel to the field **F**. The wave functions $\psi(t)$ in the rotating system are related to the wave functions in the fixed system as follows:

$$\psi'(t) = e^{iL_z\Omega t/\hbar}\psi(t) \tag{6.1}$$

where L is the orbital angular momentum operator.

Substituting (6.1) in the Schrödinger equation, we obtain

$$i\hbar\frac{\partial\psi}{\partial t} = (\hat{\mathcal{H}}_0 + d_xF - \hbar L_z\Omega)\psi' \equiv (\hat{\mathcal{H}}_0 + \hat{V})\psi. \tag{6.2}$$

so that both the electrostatic (dxF) and the "magnetic" ($L_z\Omega$) interactions are present in the rotating system, and the latter are wholly due to rotation.

The problem is thus reduced to the determination of the energy levels and wave functions of the atom in mutually perpendicular electric and magnetic fields. The solution of this problem is based on the utilization of the additional constant of motion in a Coulomb field, namely, the Runge–Lenz vector[15]

$$\mathbf{A} = \frac{1}{2m}([\mathbf{p}\times\mathbf{L}] - [\mathbf{L}\times\mathbf{p}]) - \frac{e^2\mathbf{r}}{r} \tag{6.3}$$

where p is the momentum of the electron. The matrix elements of **A** for states with fixed principal quantum number are equal to the matrix elements of the position vector: $\mathbf{r} = (-\frac{3}{2})(na_0/\hbar)\mathbf{A}$.

We now introduce the new angular momentum and frequency operators $\mathbf{J}_1, \mathbf{J}_2$ and ω_1, ω_2, defined by

$$\mathbf{J}_{1,2} = \frac{\mathbf{L}\pm\mathbf{A}}{2}; \quad \omega_{1,2} = \Omega \pm \frac{B}{e}\mathbf{F}. \tag{6.4}$$

where $B = 3ne^2a_0/2\hbar$. The operators $\mathbf{J}_1, \mathbf{J}_2$ satisfy the usual commutation rules for angular momentum.

Substitution of (6.4) in (6.2) yields

$$V = \hbar(\mathbf{J}_1\omega_1 + \mathbf{J}_2\omega_2). \tag{6.5}$$

The wave functions $u_{nn'n''}$, which diagonalize the perturbation (6.5), must obviously correspond to a definite component of $\mathbf{J}_1$ along ω_1 (represented by the quantum number n') and a component of $\mathbf{J}_2$ along ω_2 (represented by n''). These functions can be obtained from the usual parabolic wave functions $u_{ni_1i_2}$ (i_1, i_2 are the quantum numbers of the projections of $\mathbf{J}_1$ and $\mathbf{J}_2$ along the vector **F**, which itself is parallel to the x axis) through simple rotations through the angles β_1 and β_2 between the vectors ω_1 and ω_2, on the one hand, and the vector **F**, on the other.[62]

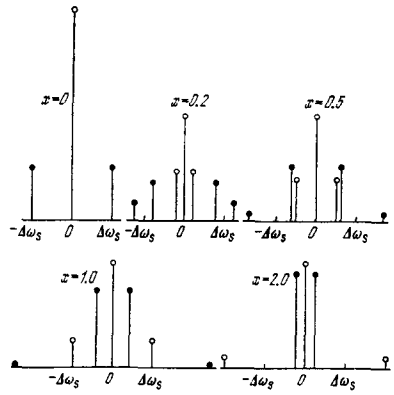

FIG. 4. The Ly-α spectrum in a rotating electric field.

The angles β_1, β_2 are determined by the ratio of the angular velocity Ω to the Stark splitting:

$$\operatorname{tg}\beta_2 = \frac{\Omega}{(B/e)F} \equiv x. \tag{6.6}$$

The wave functions $u_{nn'n''}$ diagonalize the Hamiltonian (6.5) and determine the change ΔE in the energy eigenvalues

$$\Delta E = (n' + n'')\hbar|\omega_{1,2}| = (n'+n'')\sqrt{1+x^2}\,\hbar\frac{B}{e}F. \tag{6.7}$$

Thus, in the rotating system, the wave function ψ' has the form

$$\psi'(t) = u_{nn'n''}\exp\left[-i(n'-n'')\sqrt{1+x^2}\,\frac{B}{e}Ft\right]. \tag{6.8}$$

Equations (6.1) and (6.8) can readily be used to determine the emission spectrum $I_{ab}(\omega)$ due to hydrogen in the rotating field due to the spontaneous transition from level a to level b.

This spectrum consists of a number of components (δ functions) and its amplitudes and phases depend on x, as indicated by (6.8) [see also (6.6)]. We note that the number of components exceeds the number of states (n^2) belonging to the given level. This is due to the appearance of additional "combination" shifts $\pm\Omega$ due to the rotation of the atomic dipole. Figure 4, which is taken from the paper by Ishimura,[65] shows the Ly-α spectrum for different angular velocities (different x). It is clear that each of the lateral components of the Ly-α line splits into two, and the central component splits into three, one of which is the unperturbed component. The intensity of the extreme components decreases with increasing distance from the center.

We have given a detailed analysis of the above model example because the real broadening problem is fundamentally similar to this example.

---

[8] This example is not purely a model. It can be realized in practice, for example, in the case of the excitation of a hydrogen atom in the field of circularly polarized laser radiation.

[9] It is assumed that the frequency Ω is very different from the transition eigenfrequencies in the atom.

Consider the collision of a charged (classical) particle with an excited hydrogen atom. The collision occurs on the plane defined by two vectors, namely, the velocity **v** and impact parameter ρ. In the course of time, the perturbing electric field **F** due to the incident particle will change in magnitude and will rotate through 180° in the collision plane. If, as above, we use the rotating system of coordinates with the x axis parallel to $\mathbf{F}(t)$, we again have the "magnetic" interaction $L_z\dot{\varphi}(t) \equiv \mu_0 H_{eff}(t)$ (μ_0 is the Bohr magneton), which is connected with rotation [see (4.9)].

It follows that, in the rotating system, the atom is in mutually perpendicular (and variable) electric and magnetic fields **F** and $\mathbf{H}_{eff} = \hbar\dot{\varphi}/\mu_0$.

We now use the symmetry properties of the hydrogen atom. To do this, we introduce the operators $\mathbf{J}_1$ and $\mathbf{J}_2$, defined by (6.4), and the frequencies

$$\omega_{1,2}(t) = \dot{\varphi}(t) \mp \frac{B}{e}\mathbf{F}(t). \tag{6.9}$$

The perturbation Hamiltonian (4.9) can now be rewritten in the form given by (6.5):

$$\hat{V}(t) = d_z F(t) + L_z\dot{\varphi}(t) = \hbar\,[\mathbf{J}_1\omega_1(t) + \mathbf{J}_2\omega_2(t)]. \tag{6.10}$$

The problem will be solved if we succeed in finding the wave functions $u_{nn'n''}$ that diagonalize this perturbation. As in the case of the rotating field, these functions correspond to definite components of $\mathbf{J}_1$ and $\mathbf{J}_2$ along ω_1 and ω_2, respectively. The difficulty is that the vectors $\omega_1(t)$ and $\omega_2(t)$ are functions of time. However, it is easily shown that the directions of the vectors ω_1 and ω_2 do not change in the collision process. Thus, direct analysis of the geometry of the collision in the collision plane shows that, for the field $F(t) = e^2/(\rho^2 + v^2t^2)$, the angle between the vector ω_2 and the x axis (which is parallel to **F**) is given by

$$\operatorname{tg}\beta_2 = \frac{\rho\omega}{B} = \frac{\Omega}{\omega}. \tag{6.11}$$

It follows that the special quantization directions in the hydrogen atom undergo a change during the collision process. The formula given by (6.11) shows that, transits within the Weisskopf radius ρ_W correspond to quantization along the electric field **F** whereas transits outside ρ_W correspond to quantization in the direction of the effective magnetic field $\mathbf{H}_{eff} \parallel \dot{\varphi}$.

The "correct" wave functions $u_{nn'n''}$ can thus be obtained from the parabolic functions $u_{ni_1i_2}$ corresponding to the quantization axis $Ox \parallel F$ by simple rotation through constant angles β_1 and β_2 (the angles between the vectors ω_1 and ω_2 and the x axis, respectively).

Since $u_{nn'n''}$ corresponds to definite components of $\mathbf{J}_1, \mathbf{J}_2$ along ω_1, ω_2, (6.9) and (6.10) yield the following expression for the change in the energy eigenvalue in the rotating system:

$$\Delta E = \hbar(n' + n'')\sigma\frac{\rho\omega}{e}F(t), \quad \sigma \equiv \sqrt{1 + (B/\rho v)^2}. \tag{6.12}$$

The wave function $\psi'(t)$ in the rotating system of coordinates is, therefore, found to have the form [compare this with (6.8)]

$$\psi'(t) = u_{nn'n''}\exp\left[-i(n' - n'')\sigma\frac{\rho\omega}{e}\int_{-\infty}^{t}F(\tau)\,d\tau\right]. \tag{6.13}$$

Hence, it follows that the evolution of the wave function is connected (as in the adiabatic model!) only with the modulus of the electric field $F(t)$. This problem is thus analogous to the adiabatic theory with suitably defined "components." Nonadiabatic effects, on the other hand, reduce to the dependence of the amplitudes of these components on the transit parameters, and to some complication in the phase factor. We note that the above diagonalization procedure can be used for all hydrogen lines.

The above analogy with the adiabatic model will, clearly, enable us to use the above results on the unification of the impact and static approaches (Chap. 2) in the general case that we are considering here. Calculation of the $Ly-\alpha$ line profile, based on (6.13), yields

$$I(\omega) = \frac{9N}{\pi}\frac{(\hbar/m)^2}{v}\left[\gamma\left(\frac{3\Delta\omega\hbar}{mv^2}\right) + \gamma\left(-\frac{3\Delta\omega\hbar}{mv^2}\right)\right](\Delta\omega^2)^{-1}; \tag{6.14}$$

where $\gamma(x)$ is a universal function defining the "variable" linewidth. As in (2.20), it can be expressed in terms of the Whittaker function[60]:

$$\gamma(x) = \frac{\pi^3}{2}\int_0^\infty \frac{dt}{t(1+t^2)}\left[k_{i\sqrt{1-t^2}-1}^2(xt) + k_{i\sqrt{1-t^2}+1}^2(xt) + 2t^2k_1^2(xt)\right]. \tag{6.15}$$

The limiting values of $\gamma(x)$ are as follows:

$$\gamma(x) \approx \begin{cases} -4\pi\ln x \equiv \gamma_{imp}, & x \ll 1, \\ 2\pi^2\sqrt{x} \equiv \gamma_{stat}, & x \gg 1. \end{cases} \tag{6.16}$$

By substituting (6.16) in (6.14), we obtain the results of the impact and static theories for $\Delta\omega \ll \Omega$ and $\Delta\omega \gg \Omega$, respectively. In the intermediate region, where $\Delta\omega \sim \Omega$ ($x \sim 1$), the function $\gamma(x)$ can be calculated numerically (Table I).

The function $\gamma(x)$ undergoes a smooth transition between impact and static limits, and the effects of phase and amplitude modulations and the nonadiabatic effect can be taken exactly into account. It is interesting to compare the results of the exact theory with the adiabatic model for the $Ly-\alpha$ line. This shows that the difference between the two functions $\gamma(x)$ does not exceed 20%. Hence, it is clear that the adiabatic model can be used for the approximate description of hydrogen line profiles, not only in the wings but also in the intermediate frequency region.

TABLE I.

x	0.01	0.03	0.05	0.1	0.2	0.3	0.5	1.0	1.5	2	3	5
$\frac{2\gamma(x)}{\pi^3}$	5.71	4.99	4.72	3.83	3.03	2.56	1.97	1.33	1.08	0.92	0.72	0.53

7. COMBINED BROADENING BY IONS AND ELECTRONS

In real plasma, the hydrogen atom experiences simultaneous broadening by both ions and electrons. The simplest picture of broadening in this case reduces to the following: hydrogen levels in the electric field F_i due to "slow" ions split into the individual Stark components which undergo impact broadening by "fast" electrons. The resulting line profile is obtained by averaging this picture over the static distribution of the ion field, $W(F_i)$, and by summing over all the Stark components.

The simplest profile of a Stark component can be obtained from the adiabatic model (§ 2) by taking the product of the static (Holtsmark) profile due to ions and the impact (Lorentz) profile due to electrons:

$$I(\Delta\omega)=\frac{1}{\pi}\int_0^\infty dF W(F)\frac{\gamma}{[\Delta\omega-(C/e)F]^2+\gamma^2}. \qquad (7.1)$$

For the central components of the lines $Ly-\alpha$, H_α, $H_\gamma, \ldots$, which do not undergo Stark splitting, the Stark constant C is zero and, as can be seen from (7.1), the broadening of these lines is entirely due to the impact interactions with electrons.

For the lateral line component ($C\neq 0$), we transform in (7.1) to the dimensionless variables $x=\Delta\omega e/CF_0$ and $y=\gamma e/CF_0$, and obtain[35]

$$I(\Delta\omega)=\frac{e}{CF_0}T_{\gamma}(x, y), \qquad (7.2)$$

where

$$T_{\gamma}(x, y)=\frac{1}{\pi}\int_0^\infty d\beta\,\mathcal{H}(\beta)\frac{y}{(x-\beta)^2+y^2}. \qquad (7.3)$$

The last two formulas can also be used for the approximate description of the resultant line profile if we interpret C and γ as the effective values of the Stark constant and the width for the line as a whole, respectively. The choice of C and γ was indicated above [see (3.10) and (5.18)]. The function given by (7.3) is tabulated in the literature.[10,35]

The adiabatic model is convenient because its results are universal, i.e., the same for all hydrogen lines. More rigorous calculations would require, firstly, the use of a more accurate distribution function $W_D(F_i)$ (see Chap. 3) and, secondly, the general expression given by (5.10) for electron impact broadening in the ion field. The combined effects of electron and ion broadening then assume the following form:

$$I_{ab}(\omega)=\frac{1}{\pi}\mathrm{Re}\int_0^\infty dF W_D(F)\sum_{\substack{\alpha,\alpha';\\ \beta,\beta'}}\sum_{\sigma}\langle\alpha|d_\sigma|\beta\rangle\langle\beta'|d_\sigma|\alpha'\rangle \times\left\langle\!\!\left\langle\alpha\alpha'\right|\left\{i\omega-\frac{i}{\hbar}[\hat{\mathcal{H}}_{0a}(F)-\hat{\mathcal{H}}_{0b}(F)]-\hat{\Phi}_{ab}\right\}^{-1}\left|\beta\beta'\right\rangle\!\!\right\rangle. \qquad (7.4)$$

In contrast to (7.2), this profile is not expressed in terms of universal functions but depends on a small number of parameters. It must be evaluated numerically on a computer for each particular line. The results of such calculations will be given in Chap. 10.

The profile given by (7.4) provides a good description of the intensity distribution over most of the line. At the same time, the simple convolution of the ion static and electron impact profiles does not take into account the following points: 1) in the distant part of the line wing, the electron broadening does not occur via the impact mechanism and 2) at the center of the line, the ion broadening is not by the static mechanism. The first of these means that the integrals in (7.1)–(7.3) are incorrect for $\Delta\omega\to\infty$ [nor is the more accurate integral (7.4)]. In fact, for large $\Delta\omega$, the main contribution to (7.3) is due to the regions $\beta\sim 1$ [maximum of $\mathcal{H}(\beta)$] and $\beta\sim x$, and this gives

$$T_{\gamma}(x, y)\sim\frac{1}{x^{3/2}}+\frac{y}{x^2}.$$

It is clear that the asymptotic behavior is determined by the second term, but it is readily shown that this term is comparable with the first term for $x\sim y^{-2}$ or $\Delta\omega\sim\Omega_e\sim v_e^2/C$, i.e., for values of $\Delta\omega$ for which broadening by electrons can no longer be regarded as impact broadening. The transition from electron impact broadening to the static broadening in the line wing must, therefore, be taken into account in (7.3). This can easily be done by replacing the (constant) impact width γ with the "variable" width $\gamma(x)$, defined in (2.20). This yields the correct asymptotic behavior for the line wing, which takes into account the transition from impact broadening to static broadening for electrons:

$$T_{\gamma}(x, y)\sim\frac{1}{x^{5/2}}\left[1-\frac{y(x)x^{1/2}}{2\pi^2}\right]. \qquad (7.5)$$

It follows from the last expression that, as x increases (i.e., as $\Delta\omega$ increases), an increasing number of particles produce static broadening. This can be conveniently described by introducing the effective number $R(\Delta\omega)$ of statically broadening particles:

$$R(\Delta\omega)=1-\frac{\gamma(\Delta\omega\,\Omega_e)}{\gamma_{\mathrm{stat}}(\Delta\omega\,\Omega_e)},\quad \gamma_{\mathrm{stat}}(z)=\frac{2\pi^2}{|z|}. \qquad (7.6)$$

In the impact region, where $\Delta\omega\ll\Omega_e$, we have $R(\Delta\omega)\approx 1$, i.e., the static particles are exclusively ions. In the static region, on the other hand, where $\Delta\omega\gg\Omega_e$, we have $R(\Delta\omega)\approx 2$, i.e., both ions and electrons can be regarded as static particles. The function $R(\Delta\omega)$ has a universal structure for all hydrogen lines in the adiabatic model. It is easily determined with the aid of the tabulations of $\gamma(x)$ (see Chap. 2).

In the nonadiabatic theory, the determination of $R(\Delta\omega)$ requires separate calculations for each line. The result of this kind of calculation for the $Ly-\alpha$ line is given in Chap. 6. For other lines, there are calculations that take into account the static character of electron broadening in the line wing (see Chap. 10).

We must now consider the line shape in the central region.[67] Here, we must take into account the fact that the ion field is not static. This is a very complicated problem mainly because the interactions between the ions and the atom are not binary. However, the overall picture of effects associated with the thermal motion of

the ions can easily be understood on the basis of the results obtained in Chap. 4. As we have seen, the main effects associated with thermal motion are the nonadiabatic effects due to the rotation of the ion field. It is previsely these effects that violate the static approximation near the line center, where, according to (4.12), the corresponding thermal corrections are proportional to $\Delta\omega^{-2}$ as $\Delta\omega \to 0$. The calculations given in Chap. 4 do not, however, take into account the electron impact broadening, the role of which for $\Delta\omega \to 0$ can, roughly speaking, be reduced to the replacement of the divergent quantity $\Delta\omega^{-1}$ by the finite quantity $(\Delta\omega + i\gamma)^{-1}$. Physically, this means that the inclusion of γ leads to a finite lifetime γ^{-1} of the atomic electron on the Stark sublevel and, if the ion field remains constant during this time, it can be regarded as static. This condition was first derived for ions by Griem *et al.*[47] and by Kudrin and Sholin[68] on the basis of intuitive considerations. However, the place of this criterion among the other static criteria (4.7) remained unclear. Their interrelation is discussed by Sholin *et al.*,[45] Kogan *et al.*,[69] and Kogan and Lisitsa.[70] We shall follow the discussion given by Demura *et al.*[67] and examine the role of the damping γ on the basis of a simple model calculation.

The foregoing discussion can readily be used to estimate the dependence of the effects associated with thermal motion on the plasma parameters at the line center ($\Delta\omega = 0$). All that needs to be done is to replace $\Delta\omega$ with $\gamma \sim N(C^2/v_e)\ln(\rho_m/\rho_W)$ is the expressions given by (4.11) and (4.12), which define the thermal corrections at the line center for $x = \Delta\omega/\Delta\omega_0 \ll 1$ [see (5.18)]. The correction $I^{(1)}(0)$ for the thermal motion is then given by

$$I^{(1)}(0) \propto \frac{1}{\Delta\omega_0} g_i^{-2/3} g_e^{-2/3} \Lambda^{-2}. \qquad (7.7)$$

where $g_e = N(C/v_e)^3$ is the electron broadening parameter and we take into account the fact that $\gamma/\Delta\omega_0 \propto g_e^{1/3}\ln(\rho_m/\rho_W) \equiv g_e^{1/3}\Lambda$. The dependence of $I^{(1)}(0)$ on the reduced mass μ of the ion-atom pair is determined by the factor $g_i = N(C/v_i)^3$, where $v_i = \sqrt{2T_i/\mu}$ is the relative velocity of the ion and atom. We note that a more rigorous calculation[71] will also give the spectral behavior of the thermal correction $I^{(1)}(\Delta\omega)$ for $\Delta\omega \lesssim \Delta\omega_0$.

The relative thermal correction δ is useful for comparison with experiment. For lines without the central components (H_β, H_δ), which have a minimum at the center, the relative correction δ is defined as the ratio of the difference between the intensities at the maximum (I_{max}) and the central minimum (I_{min}) to I_{max}:

$$\delta = \frac{I_{max} - I_{min}}{I_{max}}. \qquad (7.8)$$

Since $I \approx I^{(0)} + I^{(1)}$, it is convenient to use the difference $\delta_R = \delta_1 - \delta_2$ for two values of the velocity v_i (i.e., two values of g_i) which contains the thermal corrections $I^{(1)}$ in a "pure form":

$$\delta_R = \delta(g_{i1}) - \delta(g_{i2}) = \frac{I^{(1)}_{min}(g_{i1}) - I^{(1)}_{min}(g_{i2})}{I^{(0)}_{max}} \propto g_e^{-2/3}(g_{i1}^{-2/3} - g_{i2}^{-2/3}) \propto T_i T_e N^{-4/3}\frac{\mu_2 - \mu_1}{\mu_1\mu_2}. \qquad (7.9)$$

In deriving (7.9), we took into account the fact that $I^{(1)}_{min} \gg I^{(1)}_{max}$, i.e., the thermal corrections provide the main contribution at the line center. Moreover, we have also taken into account the fact that, according to (3.8), $I_{max} \sim e/CF_0$ and $v_i^2 = 2T_i/\mu$.

The expressions given by (7.7) and (7.9) define the dependence of the thermal corrections on the plasma concentration N and the reduced mass μ. We also note that δ_R is directly related to the ion temperature T_i.

Analysis of (4.11) will show that, when electron impact broadening is taken into account, the static (Holtsmark) theory for ions can also be applied to the central part of the line. For this, we require that the second term in (4.11), which is equivalent to (7.7) at the line center, should be small in comparison with the first, and this is so when

$$g_i^{2/3} g_e \Lambda^3 \gg 1, \quad \text{or} \quad \frac{\rho_{eff}\gamma}{v} \gg 1. \qquad (7.10)$$

The static condition given by (7.10) clearly shows that the "lifetime" γ^{-1} of the atom on a Stark sublevel must be small in comparison with the characteristic time for a change in the ion field (ρ_{eff}/v). The quantity ρ_{eff} is practically equal to the mean distance between the particles $N^{-1/3}$. The static condition (7.10) is thus found to augment the criterion given by (4.7) at the line center ($\Delta\omega \ll \Delta\omega_0$).

8. BROADENING OF LINES DUE TO HYDROGEN-LIKE IONS

The particular properties of the broadening of the lines of hydrogen-like ions are connected with the attraction or repulsion between the radiating ion and the perturbing charged particle in the plasma (ion or electron).

It follows from (3.3) that, to determine the static line profile due to the plasma ions, we must know the distribution function $W_i(F)$ for the static ion field in the plasma near the radiating charge. Calculations of this distribution function must, of course, take into account the repulsion of ions by the radiating center.

Let us consider the repulsion effect in the case of a radiating ion interacting with one (nearest) perturbing ion. If there were no Coulomb repulsion between the ions, the distribution function would be identical with the binary limit of the Holtsmark function (3.7), i.e., $\mathcal{H}(\beta) \approx 1.496^{-5/2}$. The main contribution to the distribution function would then be due to distances $r_{\Delta\omega}$ for which condition (3.1) is satisfied:

$$\Delta\omega = \frac{C}{e}F_{\Delta\omega} = \frac{C}{r^2_{\Delta\omega}}, \quad r_{\Delta\omega} = \sqrt{\frac{C}{\Delta\omega}}. \qquad (8.1)$$

When repulsion is taken into account, the distribution function $\mathcal{H}(\beta)$ is found to be multiplied by the Boltzmann factor $\exp[-V(r)/kT] = \exp(-e^2/rkT)$, which represents the repulsion potential. If we substitute $r = r_{\Delta\omega} = \sqrt{C/\Delta\omega}$, we see that the distortion of the distribution function is governed by the parameter $e^2/r_{\Delta\omega}kT \sim (r_0/\rho_D)^2\beta^{1/2}$, where we have introduced the following characteristic param-

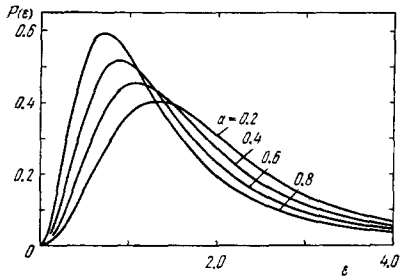

FIG. 5. The electric field distribution $P(\varepsilon)$ due to the plasma ions near a radiating charged center.

eters: the mean interparticle distance $r_0 \sim N^{-1/3}$ and the dimensionless frequency shift $\beta = \Delta\omega/CN^{2/3}$. Calculations by Margenau and Lewis,[72] based on this scheme, lead to the following expression for the binary distribution function:

$$\mathcal{W}_i(\beta) = \frac{1.496}{\beta^{5/2}} \exp\left[-0.334\left(\frac{r_0}{\rho_D}\right)^2 \beta^{1/2}\right], \tag{8.2}$$

where r_0 is given by the condition $(4/15)(2\pi)^{3/2} N r_0^3 = 1$.

More detailed calculations of $W_i(F)$ were performed by Mozer and Baranger[38] and, more recently, by Hooper.[36] Figure 5, which is taken from the paper by Hooper,[36] shows a graph of $W_i(F)$ for different values of the parameter α, defined by (3.13). It is clear that, when repulsion is taken into account, the result is a reduction in the probability of strong fields, i.e., in the intensity emitted in the line wing. The particular feature of $W_i(F)$ is the more complicated dependence on the plasma concentration N as compared with the Holtsmark case. The static ion spectra are less convenient for the determination of the plasma concentration than the spectra of neutral hydrogen. We also note that the ion spectra are much narrower than the hydrogen spectra because of the reduction in the dipole moment of the ion by the factor z.

Static broadening of the lines due to hydrogen-like ions is not confined to low-temperature plasma. An interesting example is provided by laser plasma in which, despite the high temperature ($T \sim 1$–10 keV), the ion concentration is so high ($N \sim 10^{22}$–10^{24} cm^{-3}) that $g_i = N(C3v_i)^3 \gg 1$ even for hydrogen-like ions with high $z \gg 1$. The character of line broadening in such plasma has been considered by Vinogradov *et al.*[73] The width of the static (Holtsmark) spectrum under these conditions is given by [compare this with (3.11)]

$$\Delta\omega_0 = 21.6\,\frac{n^2 Ry}{z}(Na_0^3)^{2/3}, \tag{8.1'}$$

where z is the charge of the radiating ion, a_0 is the first Bohr radius, and n is the principal quantum number of the level under consideration. Vinogradov *et al.*[73] have found the range of values of N and z for which (8.1′) can be used in plasma diagnostics.

To calculate the broadening of the ion lines by electrons, we must take into account their attraction to the radiating center. This attraction ensures that the electron moves not along a straight line (as in the field of the neutral atom) but over a hyperbola. This produces a definite complication, but it is not difficult to see that, even in this case, one can use the four-dimensional symmetry of the hydrogen-like ion. In fact, since the electron moves in the central Coulomb field of the ion, its angular momentum l is conserved ($\hbar l = mr^2\dot{\varphi}$), so that

$$\dot{\varphi}(t) = \frac{\hbar l}{mr^2(t)}. \tag{8.3}$$

This clearly shows that the instantaneous angular velocity $\dot{\varphi}(t)$ depends on $r(t)$ in the same way as the electric field $F(t)$ due to the electron, i.e.,

$$F(t) = er^{-2}(t) = \frac{me}{\hbar l}\dot{\varphi}(t). \tag{8.4}$$

This means that, as in the case of the neutral hydrogen, transformation to the rotating system of coordinates with the x axis parallel to $\mathbf{F}(t)$ (see Chap. 6) results in the appearance of mutually perpendicular electric $[\mathbf{F}(t)]$ and magnetic $[\mathbf{H}_{eff}(t) \propto \dot{\varphi}(t)]$ fields, which are in phase $[H_{eff}(t)/F(t) = \text{const}]$. This means that the hydrogen-like ion also has a special quantization direction, i.e., that of $\omega_{1,2}(t)$, which is defined as above [see (6.4) and (6.11)] by the vector sum (difference) between the electric and magnetic fields.

The above fact enabled Green *et al.*[74,75] to develop a theory of broadening of the lines of hydrogen-like ions without using the impact or static approximations. As in the case of the hydrogen atom, the temporal evolution of the wave function of the ion is determined by the phase factor $\exp[i(C/e)\int_0^t F(\tau)d\tau]$ or, according to (8.4), by the factor $e^{i\varphi(t)}$, where

$$\varphi(t) = \varphi_0 + \rho v_\infty \int_0^t \frac{d\tau}{r^2(\tau)} \tag{8.5}$$

is the rotation of $\mathbf{F}$ in the time t (φ_0 is the initial angle, v_∞ is the velocity of the electron at infinity, and ρ is the impact parameter).

In contrast to the rectilinear case, the angle φ at infinity in the case of motion on a hyperbola is bounded by $\varphi(\infty) = \arccos(1/\varepsilon)$, where $\varepsilon = [1 + m^2\rho^2 v_\infty^4/(z-1)^2 e^4]^{1/2}$ is the eccentricity of the hyperbola. Hence, it is clear that the motion becomes close to rectilinear as the velocity increases, i.e., as the plasma temperature increases.

It is clear from physical considerations that the attraction of the electron to the radiating ion should lead to an increase in the intensity in the static wing of the line, which corresponds to close encounters. Moreover, it is clear which parameter determines this effect. In fact, the new characteristic length of the problem, which is connected with the interaction between the electron and the ion is obviously the Coulomb length $\rho_k \sim e^2/mv^2 \sim e^2/kT$. On the other hand, the characteristic distance $r_{\Delta\omega}$, which determines the contribution to static broadening, is shown by (8.1) to be $r_{\Delta\omega} = \sqrt{C_i/\Delta\omega}$, where $C_i = ez_i/\hbar$ is the Stark constant of the hydrogen-like level

of the ion (ez_i is the dipole moment of the ion along the direction of the electric field of the electron). It follows that the parameter that governs the change in the intensity in the static wing of the line is the ratio of the above two lengths, i.e., $\rho_k/r_{\Delta\omega}$. When $\rho_k/r_{\Delta\omega} \ll 1$, the curvature of the trajectory can be neglected, whereas, for $\rho_k/r_{\Delta\omega} \gg 1$, it has an important effect on the nature of the spectrum. Hence, it is clear that the distribution of intensity in the line wing in the case of the ion differs from the well-known distribution (2.18) for the atom by the presence of the correcting factor $\chi(\rho_k/r_{\Delta\omega})$ which is a function of the parameter $\rho_k/r_{\Delta\omega}$. The function χ has been calculated[74,75] by a method analogous to that described in Chap. 2 [see (2.10)–(2.12)]. The resulting line profile is

$$I(\omega) = 2\pi^2 N \left|\frac{e^2 z_i}{\hbar}\right|^{3/2} \Delta\omega^{-3/2} \chi\left[\left(\frac{e^2}{kT}\right)^{1/2}\left(\left|\frac{\hbar\Delta\omega}{z_i e}\right|\right)^{1/4}\right], \quad (8.6)$$

$$\chi(x) = e^{x^2}\operatorname{erfc}(x) \to \frac{2}{\sqrt{\pi}} x \approx \begin{cases} 1, & x \ll 1, \\ \dfrac{2}{\sqrt{\pi}} x, & x \gg 1. \end{cases} \quad (8.7)$$

When $x \ll 1$, (8.6) and (8.7) yield the well-known distribution in the line wing: $I(\omega) \propto \Delta\omega^{-5/2}$ [see (2.18)]. When $x \gg 1$, (8.6) and (8.7) lead to $I(\omega) \propto \Delta\omega^{-9/4}$. It follows that, as expected, attraction between the perturbing, electron and radiating ion leads to a slower reduction in the line-wing intensity as compared with the case of neutral hydrogen. It is important to note, however, that, in practice, the region of electron static broadening in the case of hydrogen-like ions is reached for frequency detuning $\hbar\Delta\omega$ comparable with kT. Green and Cooper[75] have performed a calculation of the $Ly-\alpha$ profile for He II.

As regards the electron-impact broadening of ion lines, Griem and Shen[8,76] have shown that this is largely the same as for the neutral atom. In particular, the electron-impact broadening operator Φ_{ab} is still given by (5.14) except that the logarithmic symbol Λ is now followed by the ratio of ρ_{max} to the Coulomb length $\rho_k = \rho_{min} = ze^2/mv^2$ [it is also necessary to take into account the reduction by the factor Z in the matrix elements given by (5.15)–(5.16)].

In conclusion, let us briefly consider the broadening of neutral hydrogen lines in high-temperature hydrogen plasma containing multiply-charged impurity ions. This situation is characteristic for the Tokamak thermonuclear installations in which the plasma parameters are $T_e \sim 1$ keV, $N_e \sim 10^{13}$–10^{14} cm^{-3}. Under these conditions, we have impact-type broadening by both electrons and ions, including multiply-charged impurity ions, i.e., $g_i = N_i(C/v_{iH})^3 \ll 1$ (v_{iH} is the relative velocity of the hydrogen atom and a multiply-charged ion of charge Z_i). Hydrogen-line broadening in this type of plasma has been considered by Abramov and Lisitsa.[77] Since the impact linewidth is $\gamma \propto 1/v$ [see (5.14)], the main contribution to broadening is provided by the slower plasma ions. Even a small percentage of multiply-charged impurity ions may then play an important role, comparable with or even greater than the role of the protons. This is quite clear if we recall that an ion of charge z_i produces Stark broadening that is greater by the factor z_i than broadening by a proton, i.e., the Stark constant C is effectively increased by a factor of z_i. Since $\gamma \propto C^2 \propto z_i^2$, even 1% impurity with $z_i \sim 10$ will produce broadening of the same order as that due to protons. The resultant impact width of a level obtained by adding together the widths due to each type of ion is given by

$$\gamma = \frac{16}{3} N_e \left(\frac{\hbar}{m}\right)^2 \frac{n^4}{v_p} \Lambda \sum_i \frac{z_i^2 N_i}{N_e}, \quad (8.8)$$

where $v_p \approx v_{iH}$ is the proton velocity, N_i is the concentration of ions of type i, and $\Lambda = \ln(\rho_D/\rho_W)$.

The sum over the ions in (8.8) gives the effective ion charge of the plasma: $z_{eff} = N_e^{-1}\sum_i N_i z_i^2$. The effective charge z_{eff} is usually determined by measuring the plasma conductivity. This means that (8.8) opens up a new and interesting possibility of determining z_{eff} from data on the Stark broadening of neutral hydrogen lines. The principal difficulty is the large Doppler broadening, and special measures must be taken to exclude it.[77]

9. QUANTUM-MECHANICAL APPROACH TO THE BROADENING PROBLEM

The essence of the classical formulation used above is that the motion of the broadening particle (say, ion) is assumed given and one considers the change in the wave function of the radiating atom. The quantum-mechanical formulation is, in a sense, the converse of this. In particular, one considers the motion of the broadening ion in the field of the radiating atom. The frequency shift $\Delta\omega$ in the emitted radiation is then related to the change in the energy of the ion, $\hbar^2 q^2/2M$:

$$\frac{\hbar^2}{2M}(q_a^2 - q_b^2) = \hbar\Delta\omega; \quad (9.1)$$

where q_a and q_b are the momenta of ions of mass M interacting with the atom in the upper (a) and lower (b) states between which the radiative transition takes place ($\omega_{ab} \equiv \omega_0$). For simplicity, we shall neglect the interaction between the ion and the atom in the lower state (b). The change in the frequency of the radiation emitted by the atom is thus related, in the quantum-mechanical formulation, to energy transfer to external degrees of freedom.

As already noted, the quantum-mechanical formulation was first discussed by Jablonski,[28] who used the quasiclassical wave functions of the broadening particle to calculate the static spectrum. The method was subsequently used by Szudy[29] and Szudy and Bailis.[30] The quantum-mechanical approach has also been used to describe impact broadening by electrons, and this has led to a relationship between the impact width and shift, on the one hand, and the electron-atom scattering cross section, on the other. This was done by Sobel'man[26] and by Baranger.[27]

Nevertheless, until quite recently, there were no published detailed calculations of line profiles based on the quantum-mechanical approach and, in particular, no calculations of this kind relating to the transition region between the impact and static limits. This was due to

the fact that the quantum-mechanical solution required knowledge of the exact wave functions of the perturbing particle and, as a rule, these could only be found through a numerical solution of the Schrödinger equation. We emphasize that, in contrast to scattering problems, the broadening problem requires knowledge of the wave function for any distance r, and not simply for the asymptotic region $r \to \infty$.

Very recently, quantum-mechanical calculations of the hydrogen $Ly-\alpha$ line were reported in a series of papers by Tran Minh *et al.* [78-80] We shall adopt a different approach, [81] based on the symmetry properties of the hydrogen atom, and will also discuss in detail the connection between the quantum-mechanical solution and the exact classical solution given in Chap. 6.

Let us begin by deriving the quantum-mechanical expression for the line profile $I_{ab}(\omega)$ due to a transition between level a and level b of the atom. The levels are assumed nondegenerate in l, and the interaction between the atom and ion in states a and b is represented by spherically symmetric potentials $U_a(r)$ and $U_b(r)$.

We shall suppose that the quantum $\hbar\omega$ is emitted by a single system consisting of the atom and the broadening ion. The wave function of this system in the initial and final states is given by the product of the wave functions of the atom, φ_a, φ_b, and the wave function $\psi^{\pm}_{qa,b}$ of the ion, describing the scattering of the particle of momentum q by the potentials U_a and U_b (the two signs $\pm$ correspond, respectively, to asymptotically converging and diverging spherical waves at infinity).

The probability of a transition of the system from state a to state b with the emission of a photon of frequency ω and momentum k is given by the following well-known expression:

$$W = \frac{2\pi}{\hbar} |\langle a | V | b \rangle|^2 \delta(\varepsilon_b - \varepsilon_a) \frac{dq_b}{(2\pi)^3} \frac{dk}{(2\pi)^3}, \qquad (9.2)$$

where V is the operator representing the interaction between the atom and the radiation field, and the wave functions $\langle a|$, $|b\rangle$ and the energy difference $\varepsilon_a - \varepsilon_b$ of the atom + ion system are given by

$$\varepsilon_a - \varepsilon_b = \frac{\hbar^2}{2M}(q_b^2 - q_a^2) - \hbar\Delta\omega, \quad |a\rangle = \varphi_a \sqrt{\frac{M}{\hbar q_a}} \psi^{+}_{q_a}, \quad |b\rangle = \varphi_b \psi^{-}_{q_b}. \qquad (9.3)$$

The wave function $|a\rangle$ is assumed to be normalized to a unit flux of the broadening particles (ions). After averaging over the initial states and summing over the final states, the expression given by (9.2) will therefore give the differential cross section $d\sigma/d\omega$ for the emission of a photon of frequency ω in the range $d\omega$. The cross section $d\sigma/d\omega$ is completely analogous to the bremsstrahlung emission cross section. There is, however, one important difference: in the bremsstrahlung case, the interaction V with the electromagnetic field includes the dipole moment of the scattering particle, whereas, in the case of broadening, it includes the dipole moment of the atom. The total radiation intensity in the case of broadening will not, therefore, depend on whether the atom scatters an ion or an electron.

It is clear from the foregoing that, to evaluate the cross section $d\sigma/d\omega$ for the emission of a photon of frequency ω by the atom, we can use the expressions for the bremsstrahlung emission cross section (see, for example, Sobel'man, [10] §34, Part 3) with the dipole moment er of the electron replaced by the dipole moment of the atom, and the wave function of the atom + ion system given by (9.3). The final result is

$$\frac{d\sigma}{d\omega} = \frac{4\omega^3 |\mathbf{d}_{ab}|^2}{3c^3} \frac{\pi^2}{v_a E_a q_b} \sum_l (2l+1) |A_l|^2; \qquad (9.4)$$

where $E_a = \hbar^2 q_a^2/2M$ and v_a are, respectively, the energy and velocity of the electron in state a. The matrix element of the dipole moment d of the atom over the wave functions of the atom + ion system is thus split into the product of the matrix element of d between states a and b of the atom and the *overlap integral* A_l for the wave functions of the ion with angular momentum l:

$$A_l = \int_0^\infty dr\, r^2 R^{(a)}_{q_a l}(r)\, R^{(b)}_{q_b l}(r). \qquad (9.5)$$

where $R^{(i)}_{qi}{}_l$ are the solutions of the radial Schrödinger equation with angular momentum l in the potentials $U_a(r)$ and $U_b(r)$.

The expression for the radiated power per unit volume per unit frequency can be expressed in terms of the cross section $d\sigma/d\omega$, as in the case of the bremsstrahlung radiation, and is given by

$$Q(\omega) = N_A N_i \hbar\omega \int v_a f(v_a) \frac{d\sigma}{d\omega} dv_a. \qquad (9.6)$$

where N_A, N_i are the concentrations of atoms and ions, and $f(v_a)$ is the distribution over the initial relative velocities. As before, we shall not average over v_a, i.e., we shall suppose that $f(v_a) \propto \delta(v_a - v_0)$ (whenever necessary, this averaging can be carried out in the last stage). Dividing (9.6) by the total intensity of radiation emitted by the atoms, $N_A 4\omega^4 |\mathbf{d}_{ab}|^2/3c^3$, we obtain the following expression for the profile emitted by an individual atom:

$$I(\omega) = N_i \frac{\pi^2\hbar}{E_a q_b} \sum_l (2l+1) |A_l|^2. \qquad (9.7)$$

Thus, in the quantum-mechanical formulation, the determination of the line profile reduces to the evaluation of the overlap integral A_l, whose dependence on the frequency shift $\Delta\omega$ is given by (9.1).

As frequently mentioned above, the particular properties of hydrogen line broadening are connected with the degeneracy of levels a and b in the angular momentum l. The main difficulty in the solution of the problem is, therefore, in taking into account the interaction of all the degenerate states of the atom during scattering of the broadening ion. We must now find the wave function $\psi(r_i)$ of the ion interacting with the excited hydrogen atom. The Hamiltonian for the system is

$$\mathcal{H} = \mathcal{H}_{0A} + \mathcal{H}_{0i} + V_{Ai}, \quad V_{Ai} = -\frac{\mathbf{r}_i \mathbf{r}_A}{r_i^3}, \qquad (9.8)$$

where $\mathcal{H}_{0A}$, $\mathcal{H}_{0i}$ are the Hamiltonians for the free atom and free ion, respectively, and V_{Ai} is the operator for their dipole interaction.

We note that the potential V_{Ai} is noncentral and, in contrast to the above case, the orbital angular momentum $\mathbf{l}_i$ of the ion is not, therefore, conserved. The conserved quantity is only the resultant angular momentum $L=\mathbf{l}_i+\mathbf{l}_A$, where $\mathbf{l}_A$ is the orbital angular momentum of the atom.

If we now write the wave function $\Psi(\mathbf{r}_A, \mathbf{r}_i)$ of the ion + atom system in the form of an expansion over products of the unperturbed wave functions corresponding to the level n of the atom, i.e., $\psi^{(n)}(\mathbf{r}_A)$, and the wave functions of the ion, $\psi(\mathbf{r}_i)$, then, after substitution into the Schrödinger equation with the Hamiltonian given by (9.8), we obtain a system of coupled equations for the functions $\psi(\mathbf{r}_i)$. This system is analogous to the system of equations with strong coupling in the theory of scattering[82] (Chap. 13), the solution of which is a relatively difficult problem. In the present case, however, we can avoid having to perform a direct solution of this problem by using the fact that, for the dipole potential defined by (9.8), there is an additional constant of motion[83,64]:

$$\Lambda = \mathbf{l}_i^2 - 2Mr_A(\mathbf{n}_i\mathbf{n}_A), \quad \Lambda\psi = \lambda\psi, \tag{9.9}$$

where $\mathbf{n}=\mathbf{r}/r$ is a unit vector in the direction of $\mathbf{r}$ (henceforth, we shall use the atomic system of units in which $e=\hbar=m=1$).

The use of wave functions with a definite eigenvalue λ is convenient because we know the solutions $R_{\lambda L}(r)$ of the equation describing the radial motion of the ion. In fact, the dipole potential V_{Ai} falls off as r_i^{-2}, i.e., in the same way as the centrifugal potential $V_{cf}=-l_i^2 r_i^{-2}$. The sum of the two potentials then contains the constant of motion Λ given by (9.9) as a coefficient of r_i^{-2}. In view of this, the radial equation for the ion has the form (the subscript i will be omitted henceforth)

$$\frac{d^2R}{dr^2}+\frac{2}{r}\frac{dR}{dr}+\left(q^2-\frac{\lambda}{r^2}\right)R=0. \tag{9.10}$$

The solution of this equation can be expressed[15] in terms of the Bessel functions:

$$R^{\lambda L}(r)=\sqrt{\frac{q}{r}}J_{\sqrt{\lambda+(1/4)}}(qr). \tag{9.11}$$

The solution thus has the same form as for the free motion of an ion except that, instead of the orbital angular momentum $l_i+(\frac{1}{2})$, the subscript on the Bessel function now contains the quantity λ which contains information on the dipole interaction between the ion and the atom.

Despite the apparently simple form of the solution given by (9.11), we must recall that, before we can use it, we must find the value of λ and the wave functions $\psi_{\lambda LM}$, i.e., we must solve the secular equation given by (9.9). The functions $\psi_{\lambda LM}$ corresponding to definite values of the total angular momentum L, its projection M, and the constant of motion λ, can be conveniently sought in the form of the expansion

$$\psi_{\lambda LM}=R^{\lambda L}(qr)\sum_{l_A l_i}a_{l_A l_i}^{\lambda L}|LMl_Al_i\rangle, \tag{9.12}$$

where the functions $|LMl_Al_i\rangle$ can be expressed in terms of the spherical harmonics Y_{lm} in the usual way (with the aid of the Clebsch–Gordan coefficients[15]).

Substitution of (9.12) in (9.9) leads to a system of algebraic equations for the coefficients $a_{l_A l_i}^{\lambda L}$, the determinant of which can be used to find the value of λ. The problem of determining λ and the coefficients $a_{l_A l_i}^{\lambda L}$ for the $n=2$ level ($Ly-\alpha$ line) has been considered by Seaton[58] in connection with scattering problems. We shall not reproduce the relevant and rather unwieldy formulas, and will suppose henceforth that the coefficients $a_{l_A l_i}^{\lambda L}$ and the values of λ are known.

Before we can use the bremsstrahlung cross section $d\sigma/d\omega$ in the evaluation of the line profile, as described above, we must relate the function $\psi_{\lambda LM}$ to the functions $\psi_{q l_0 m_0}^{\pm}$ which contain the incident plane wave and diverging (and converging) spherical waves:

$$\psi_{\mathbf{q}l_0m_0}^{\pm}\underset{r\to\infty}{\sim}\varphi_{l_0m_0}e^{i\mathbf{qr}}+\frac{f^{\pm}}{r}e^{\pm iqr}, \tag{9.13}$$

where $\varphi_{l_0m_0}$ is the wave function of the atom in the state l_0m_0.

This relationship can be established with the aid of the expansion

$$\psi_{\mathbf{q}l_0m_0}^{\pm}=\sum_{\lambda LM}d_{\lambda LM}^{(\pm)l_0m_0}\psi_{\lambda LM}, \tag{9.14}$$

where the coefficients $d_{\lambda LM}^{(\pm)l_0m_0}$ can be obtained by demanding that the functions given by (9.13) and (9.14) must be equal as $r\to\infty$.

Proceeding as in the derivation of (9.4)–(9.7), we substitute the functions $\psi_{q l_0 m_0}^{\pm}$ into the general formulas for the cross section $d\sigma/d\omega$ for the emission of a photon of frequency ω, and obtain the following expression for the line profile connected with the transition from level n to a nondegenerate lower level:

$$I(\omega)=\frac{\pi^2\hbar N_i}{3E_aq_b}\sum_{\lambda,L}(2L+1)[(a_{1L-1}^{\lambda L}A_{LL}^{L-1})^2+(a_{1L+1}^{\lambda L}A_{LL}^{L+1})^2]. \tag{9.15}$$

Comparison of (9.15) with the expression for the two-level approximation given by (9.7) shows that transitions with a change in the angular momentum l_i of the ion by ±1 contribute to the profile with weights given by the coefficients $a_{l_A l_i}^{\lambda L}$ [see (9.12)]. Moreover, the profile includes contributions of all scattering channels corresponding to different values of the constant of motion λ.

Further investigation of (9.15) involves an analysis of the radial overlap integrals $A_{\nu_a\nu_b}$, which, according to (9.11), have the form

$$A_{\nu_a\nu_b}=\sqrt{q_aq_b}\int_0^\infty dr\,rJ_{\nu_a}(q_ar)J_{\nu_b}(q_br). \tag{9.16}$$

where ν_a, ν_b are related to λ in a simple fashion (9.11).

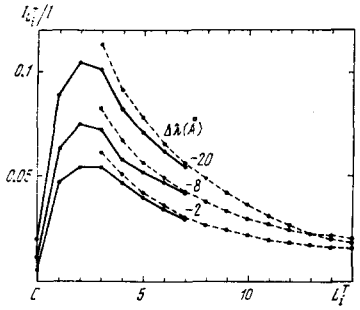

FIG. 6. Relative contribution of angular momenta L_i^T to the electron profile $I(\Delta\lambda)$ of the Ly-α line for different distances $\Delta\lambda$ from its center.

The overlap integral given by (9.16) can be expressed in terms of the complete hypergeometric function

$$F\left[\frac{\nu_a+\nu_b}{2},\ \frac{\nu_a-\nu_b}{2},\ \nu_a,\ 1,\ \left(\frac{q_a}{q_b}\right)^2\right],$$

where, according to (9.1), the dependence on the frequency detuning $\Delta\omega$ is given by

$$\left(\frac{q_a}{q_b}\right)^2=\left(1+\frac{2M\Delta\omega}{q_a^2}\right)^{-1}. \tag{9.17}$$

The profile given by (9.15) is thus seen to admit of a direct analytic evaluation. The question arises as to what is the relationship between the quantum-mechanical solution and the exact classical solution given in Chap. 6. It turns out that this can be established by direct limiting transition in (9.15) and (9.16) to high angular momenta L:

$$L\gg\sqrt{\frac{3}{2}n(n-1)M}. \tag{9.18}$$

If we recall that $L=Mv\rho$, we find that the quantum-mechanical expression (9.15) and the classical expression given by (6.15) become identical for the $Ly-\alpha$ line. Analysis of this limiting transition enables us to establish the criteria for the validity of the classical approximation. In the impact region ($\Delta\omega C/v^2\ll 1$), the effective impact parameter ρ_{eff} (and, consequently, $L_{eff}=Mv\rho_{eff}$) is determined by the Weisskopf radius $\rho_W\sim C/v$ (see Chap. 2), so that condition (9.18) yields

$$\sqrt{CM}\gg 1. \tag{9.19}$$

In the static region ($\Delta\omega C/v^2\gg 1$), we have $\rho_{eff}\sim r_{\Delta\omega}=\sqrt{C/\Delta\omega}$ [see (8.1)], so that (9.18) reduces to

$$\Delta\omega\ll Mv^2. \tag{9.20}$$

This condition has an obvious interpretation: the change $\hbar\Delta\omega$ in the particle energy during the interaction with the atom is small in comparison with its initial energy.

It follows from (9.19) and (9.20) that the classical approach is valid for sufficiently high lines (high values of the Stark constant C), heavy particles ($M\gg 1$), and not too distant line wings ($\Delta\omega\ll Mv^2$). We note that the quantum-mechanical effects can be important in the line wing for both electrons and ions, since the usual situation in plasma corresponds to $Mv_i^2\sim mv_e^2\sim kT$.

The dipole approximation is not valid for the distant line wings. Moreover, the inclusion of quadrupole corrections is usually insufficient and the exact potential must be employed.

Feautrier *et al.*[80] have carried out detailed calculations of the $Ly-\alpha$ line profile for the case of electron broadening. Figure 6 shows the relative contribution of the angular momenta L to the electron profile of the $Ly-\alpha$ line for different distances $\Delta\lambda$ from its center. It is clear that the dipole approximation for $L\sim 5-6$ differs from the exact result by 10–15%. The contribution of low angular momenta $L<3$, which are not taken into account in the dipole approximation, is particularly appreciable in the line wing (for $\Delta\lambda=20$ Å, this contribution amounts to 30%, and for $\Delta\lambda=60$ Å, it is roughly 50%). For $\Delta\lambda\gtrsim 60$ Å, we must even take into account electron exchange effects.

10. NUMERICAL CALCULATIONS AND COMPARISON WITH EXPERIMENT

Calculations of line profiles based on the general formulas given by (7.4) involve laborious numerical calculations. Such calculations have been carried out in recent years by Keple and Griem[84] and by Vidal *et al.*[85] for the initial lines of the Lyman and Balmer series. They used microfield distributions $W_D(F)$ including ion correlation (Chap. 3), and the electron velocity distribution was assumed to be Maxwellian. The calculation by Vidal *et al.*[85] were based on the so-called generalized theory of broadening which took into account the transition from the electron impact broadening to the static broadening in the line wing.

It is important to note that the above two calculations suffer from a discrepancy which is particularly large (~30–40%) in the central parts of lines with unshifted components (H_α, H_β). These discrepancies are largely due to the particular choice of the logarithmic cutoff parameters in the impact width (5.13), and the way in which the nondiagonal matrix elements of the operator Φ_{ab} were taken into account [see (5.16)]. In the region of the order of the half-width and in the line wings, this discrepancy is much smaller. For lines without central components (H_β, H_δ), the discrepancy is also small (~5–10%).

Figures 7–10 show the results of experiments performed by Wiese *et al.*[86] and the numerical calculations for four hydrogen lines belonging to the Balmer series. It is clear that the observed and calculated profiles are quite close to each other, except for the line center where the discrepancy is particularly appreciable for lines with central components (H_α, H_γ). The agreement between theory and experiment is somewhat better for lines without central components (H_β, H_δ). However, in the central parts of the lines, the observed intensity is always higher than the calculated intensity. This is probably connected with the thermal motion of the ions, which is not taken into account in the calculations (see below).

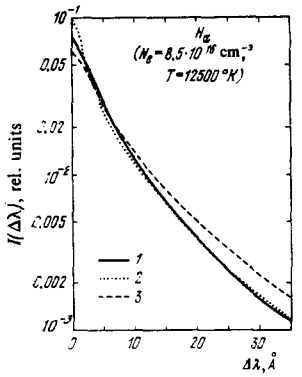

FIG. 7. The H_α profile: 1—experiment,[86] 2—calculation,[84] 3—calculation.[85]

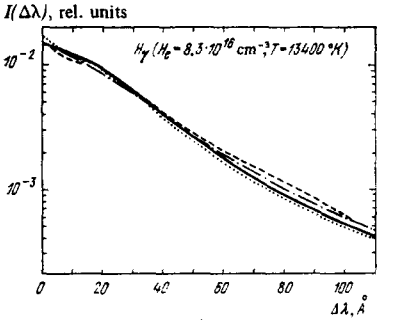

FIG. 9. The H_γ profile: the notation is the same as in Figs. 7 and 8.

The role of electrons in broadening is particularly appreciable for lines with an unshifted Stark component (H_α, H_γ). The structure of such lines consists of a strong central component, whose broadening is wholly due to the electron impact interaction, and weaker lateral components broadened by the static ion interaction.

For lines without central components ($Ly-\beta, H_\beta, H_\delta$), the influence of electrons on the central part of the profile is somewhat smaller (see Figs. 8 and 10). However, even here the contribution of electron broadening is appreciable. Thus, in the absence of impact broadening by electrons, the static line profile due to ion broadening should have zero intensity at the line center, where $\Delta\omega = 0$ [see, for example, (7.1)]. When electron broadening is taken into account, on the other hand, the central valley turns out to be much smaller for such lines (see Figs. 8 and 10).

It is important to note that electrons affect not only the central part of a line, but also the distant wings that are not shown in Figs. 7–10. These wings correspond to static broadening by both ions and electrons. According to the general results of the theory of broadening (Chaps. 2 and 7), static broadening by electrons should be seen for $\Delta\omega \propto v_e^2/c = \Omega_e$. This region can be observed either in the distant wings of lines (for initial lines belonging to the Lyman and Balmer series) or for highly excited levels for which the Stark constant $C \propto n^2$ is sufficiently large (Ω_e is small). Both these possibilities have been realized experimentally. The distant wings of the $Ly-\alpha$ line have been observed by Boldt and Gooper[87] and by Elton and Griem.[88] Highly excited lines of the Balmer series (H_8-H_{15}) have been observed by Schluetter and Avila.[89,90] The results of both types of experiment can be conveniently expressed in terms of the relative number R of statically broadening particles [see (7.6)]. Figure 11 shows the results obtained by Boldt and Gooper[87] for the wing of the $Ly-\alpha$ line, together with the results of theoretical calculations.[17,91,92] It is clear that, as one moves further into the wing, the fraction of electrons producing static broadening increases. For $\Delta\lambda \sim 50$ Å, the effect of practically all the particles can be described by the static theory ($R \approx 2$).

In Schlütter's experiments,[90] the boundary $\Delta\lambda_L$ of the transition to the static broadening for electrons is satisfactorily described by the formula

$$\Delta\lambda_L = \frac{0{,}62 \cdot 10^{12} c_e^2 \lambda^2}{n(n-1)}. \qquad (10.1)$$

According to the static theory, the intensity distribution in the wing should be

$$I(\Delta\lambda) \propto R(\Delta\lambda)^{-m}. \qquad (10.2)$$

where $R \approx 2$ is the relative number of statically broadening particles and the exponent is $m = \frac{5}{2}$.

Figures 12 and 13 show the observed values of R and m as functions of the principal quantum number n of the upper level. These values are close to the theoretical predictions. Figure 14 shows the observed line profile for H_{15} together with the value of $\Delta\lambda_L$. It is clear from (10.1) that, in the case of highly excited lines, the electrons begin to broaden statically even at the line half-width. Figure 15 shows a plot of $R(\Delta\lambda/\Delta\lambda_L)$ for the H_{15} line. As can be seen, the agreement between measurement and theory is satisfactory.

Let us now consider the behavior of the hydrogen line profile near the line centers. Experiments with the H_β

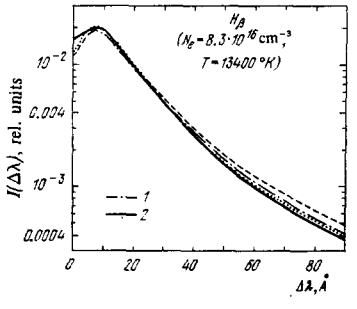

FIG. 8. The $H\beta$ profile: the notation is the same as in Fig. 7. 1—"Red" wing, 2—"blue" wing.

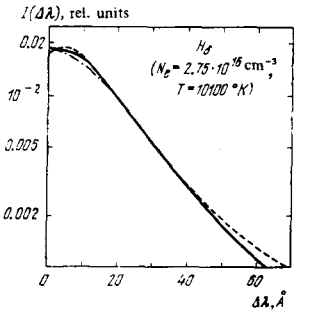

FIG. 10. The H_δ profile. the notation is the same as in Figs. 7–9.

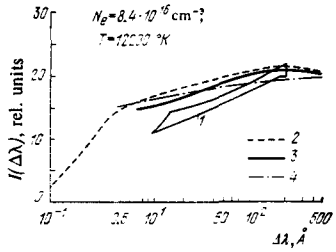

FIG. 11. Profile of the Ly-α line in the distant wing: 1—experiment,[87] 2—calculation,[91] 3—calculation,[92] 4—adiabatic model.[17]

line, which does not have a central component, have shown, as already noted, that the central intensity is systematically higher than the calculated value. In recent experiments, Wiese *et al.*[93-94] have shown that this difference depended on the reduced mass μ of the radiating atom and the perturbing ion. The observed reduced-mass effect is shown in Fig. 16 for the broadening of hydrogen atoms (H) and deuterium atoms (D) by H^+, D^+, and Ar^+ ions (reduced masses $\mu_{HH}=0.5$, $\mu_{HAr}=1$, and $\mu_{DAr}=1.9$). It is clear that, as μ increases, the valley at the center of the H_β is also increased. This effect is obviously due to the reduction in the thermal motion of the ions as the reduced mass μ increases. Calculations relating to these observations have been undertaken,[95-98] but an exhaustive explanation of the effect is still lacking. We shall try to give below a qualitative description of the thermal motion effect, using the results given in Chap. 7 [see Eq. (7.7)]. Figure 17 shows the depth of the valley at the center of the H_β as a function of the perturbing ions.[67,71] Although the agreement between experiment and theory is quite good, the experimental data are not good enough to distinguish between the $1/\mu$ and $1/\sqrt{\mu}$ dependence.

The H_α and H_γ lines, which have central components, are also found to exhibit the "reduced-mass effect."[94] Figure 18 shows the H_α profile for two values of μ. It is clear that an increase in the velocity of thermal motion (reduction in μ) leads to a reduction in the intensity

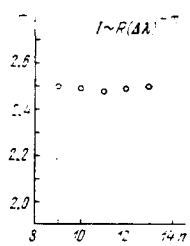

FIG. 12. Exponent m defining the reduction intensity in the line wing for the higher Balmer line (Schlütter's data[90]).

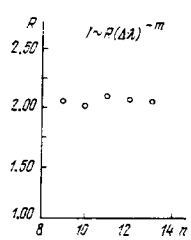

FIG. 13. Relative number R of statically broadening particles for the wings of the highly excited Balmer lines (Schlütter's data[90]).

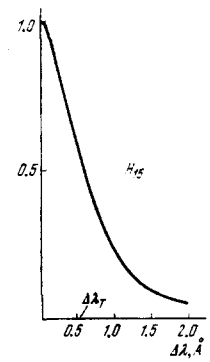

FIG. 14. Observed[90] H_{15} profile. $\Delta\lambda_T$ indicates the boundary of the static region for electrons.

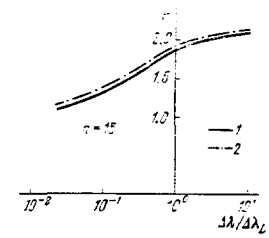

FIG. 15. Plot of $R(\Delta\lambda)$ for the H_{15} line: 1—Schlütter's data,[90] 2—calculations based on the adiabatic model.[17]

of the line at the maximum and to a certain increase in its half-width. This can be understood in a general way because any additional perturbation of the atom (including the motion of the ion) should lead to an additional broadening of the line and, consequently, to a reduction in the central intensity because of normalization. However, additional calculations will be required before this effect can be explained quantitatively.

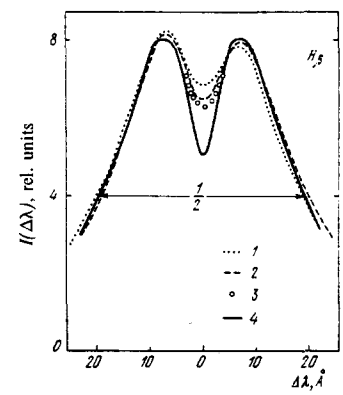

FIG. 16. The "reduced mass effect" for the H_β (Wiese *et al.* experiment[93,94]): 1—H–H$^+$ ($\mu=0.5$), 2—H–Ar$^+$ ($\mu=1$), 3—D–Ar$^+$ ($\mu=2$), 4—theory $N_e=8\times10^{16}$ cm^{-3}.

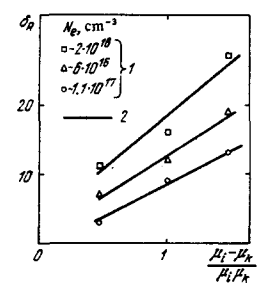

FIG. 17. Depth δ_R of valley at line center as a function of the reduced mass μ of the atom-ion pair: 1—experiment by Weise *et al.*,[93,94] 2—calculation.[67]

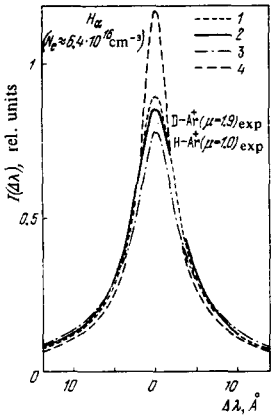

FIG. 18. The "reduced mass effect" for the H_α (experiments by Wiese *et al.*[94]): 1—D–Ar$^+$ (μ =1.9), 2—H–Ar$^+$ (μ=1.0), 3—calculation,[84] 4—calculation.[85]

It is important to note that, from the standpoint of general principles, the "reduced-mass effect" forces us to generalize the theory of broadening to the case where the interaction between the ions and the atom can no longer be looked upon as static or binary. This corresponds to $g_i \sim 1$ and presents great computational problems.

The last effect that we must touch upon is connected with the asymmetry of the hydrogen lines observed in dense plasma (see Figs. 8 and 10; the "blue" and "red" line wings). Calculations of this asymmetry performed by Kudrin and Sholin,[68] Sholin,[99] Müller,[100] and recently by Demura and Sholin[101] have shown that effects connected with the inhomogeneity of the ion field play the dominant role here. In fact, all the above calculations were based on the inclusion of only the dipole interaction between the atom and the ion field F_i. Higher-order terms correspond to the interaction between the quadrupole moment Q_{ml} and the field gradient ∇F_i:

$$\hat{V} = -\frac{1}{6} Q_{ml} \frac{\partial (F_i)_m}{\partial x_l}. \tag{10.3}$$

When the interaction given by (10.3) is taken into account, the result is a modification of the wave functions and energy eigenvalues of the atom obtained for a fixed ion field. The profile of the Stark line component corrected for ion field inhomogeneity has the form[101]

$$I(\Delta\omega) = \int_0^\infty d\beta \frac{\gamma}{(\Delta\omega - CF_0\beta/e)^2 + \gamma^2} \left\{ \mathcal{H}(\beta) + \frac{n^2 a_0}{2R_0} [a_1 \Lambda(\beta) + a_2 \chi(\beta)] \right\}, \tag{10.4}$$

where C is the Stark constant, γ is the impact width of the component, $R_0 = (3/4\pi)^{1/3} N^{-1/3}$ is the mean interparticle distance, and $n^2 a_0$ is the size of the atom. The functions $\Lambda(\beta)$ and $\chi(\beta)$ describe the influence of inhomogeneity on the amplitude and energy of the Stark states, respectively:

$$\Lambda(\beta) \propto \begin{cases} \beta^{-2}, & \beta \gg 1, \\ \beta^3 & \beta \ll 1, \end{cases} \tag{10.5}$$

$$\chi(\beta) \propto \begin{cases} \beta^{-2}, & \beta \gg 1, \\ -\beta^3, & \beta \ll 1 \end{cases} \tag{10.6}$$

where a_1 and a_2 are numerical constants that depend on the chosen line.

It is clear from (10.4) that the correction for the nonuniformity of the ion field is determined by the parameter $n^2 a_0/R_0$. The influence of nonuniformity increases with increasing ion field $\beta = F/F_0$, i.e., with decreasing distance between the perturbing ion and the radiating atom. This follows from an analysis of the behavior of the functions $\Lambda(\beta)$ and $\chi(\beta)$ given by (10.5) and (10.6). In particular, when $\beta \ll 1$, the corrections decrease more rapidly ($\propto \beta^3$) than the zeroth (Holtsmark) profile ($\propto \beta^2$). On the other hand, when $\beta \gg 1$, these corrections decrease more slowly [$\propto \beta^{-2}$ as compared with $\mathcal{H}(\beta) \propto \beta^{-5/2}$]. The result given by (10.4) is, therefore, restricted by the range of validity of perturbation theory and is itself valid only for values of β that are not too high or, more precisely, for

$$\beta \ll \left(\frac{R_0}{3n^2 a_0}\right)^2. \tag{10.7}$$

We note that, when $N \sim 10^{17}$ cm^{-3} and $n = 4$, the Holtsmark profile is valid right up to $\beta \approx 30$. For the lateral component of the $Ly-\alpha$ line, the criterion given by (10.7) is satisfied up to distances $\Delta\lambda \sim 50$ Å from the line center.

Condition (10.7) is a further restriction on the validity of the Holtsmark theory and thus joins (4.7) and (3.14) [see above for a discussion of this question before Eq. (4.13)].

We note in conclusion that there is one further reason for the asymmetry of lines, namely, ionization (burnup) of Stark components in the strong electric field due to the ions in dense plasma. It was shown in[102] that this effect could be taken into account by multiplying the intensity of the line component by the factor $A/[A + j(F)]$, where A is the probability of spontaneous decay and $j(F)$ is the probability of ionization of the component. It is well known[103] that components shifted toward longer wavelenghts ("red" component) tend to burn up more rapidly than the "blue" components. The static line profile will therefore have a stronger "blue" wing. The burnup effect becomes appreciable for highly excited lines (H_γ, H_δ) at plasma densities $N \gtrsim 10^{18}$ cm^{-3}.

11. CONCLUSIONS

In conclusion, we must try to formulate some simple practical recipes for estimating the broadening of hydrogen lines in plasma. The first step is to estimate the density N, the characteristic velocities v_i and v_e of the plasma ions and electrons, and the magnitude of the Stark constant C for the given line [see (3.10)]. To establish the character of the broadening by ions and electrons, we must next estimate the parameters g_i and g_e [see (2.7)]. If $g \ll 1$, the broadening is largely due to the impact mechanism and, if $g \gg 1$, we are dealing mainly with static broadening. If $g_i \ll 1$ and $g_e \ll 1$, the linewidth can be calculated from the impact theory, i.e., from (5.18), and is obviously mainly determined by the heavier particles, i.e., ions. For $g_i \gg 1$ and $g_e \gg 1$, both particles produce static broadening and the linewidth can be estimated from (3.11) by substituting $N_{eff} = N_i + N_e = 2N$ into it. Usually, broadening by ions is static ($g_i \gg 1$), whereas broadening by electrons is of

the impact type ($g_e \ll 1$). If this is so, then for the lateral components ($C \neq 0$), the ion width $\Delta\omega_{0i} \sim \lambda C N^{2/3}$ is greater than the electron width $\gamma_e \sim NC^2 \ln(\rho_D/\rho_W)/v_e$ because $\gamma_e/\Delta\omega_{0i} \sim g_e^{1/3} \ll 1$. For the central component ($Ly-\alpha$, H_α, H_γ), the linewidth is determined by only the electron impact broadening mechanism. This completes the list of integrated (over the spectrum) line-broadening and linewidth estimates.

When line shapes are estimated in different regions of $\Delta\omega$, one must remember the following two points: 1) even for $g \ll 1$, impact broadening in the line wing is replaced by static broadening for $\Delta\omega \gtrsim \Omega \sim v^2/c$, and 2) even for $g \gg 1$, the static approximation is violated in the central part of the line, where $\Delta\omega \lesssim \sqrt{CNv}$ [see (4.7)]. We recall that the static criterion (4.7) itself has a different form for $g \ll 1$ and $g \gg 1$. In the case of combined electron and ion broadening, the static approximation may turn out to be valid for ions even at the line center provided (7.10) is satisfied. The most difficult case is that corresponding to $g \sim 1$, where the impact and static mechanisms predict linewidths of the same order. Here, the behavior of the line profile is clear only in the region corresponding to its static wing. Finally, we note that all the above estimates correspond to the ideal plasma approximation (3.14) and the uniform microfield approximation (10.7).

The accuracy of existing results on the line profiles is very dependent on the particular plasma parameters and the particular spectral lines. In practice, the most interesting case is that of static ions ($g_i \gg 1$) and impact electrons ($g_e \ll 1$). This is considered below.

The simplest line profile (7.1)–(7.3) with the average Stark constant C given by (3.10) and impact width γ given by (5.15)–(5.16) gives reasonable precision (~30%) in the neighborhood of the line half-width, i.e., for $\Delta\omega \sim \Delta\omega_0$ [see (3.11)]. However, the profile may differ quite substantially from the true situation in the central part, where $\Delta\omega \ll \Delta\omega_0$, and in the wings, where $\Delta\omega \gg \Delta\omega_0$.

A correct description of the line wing can only be achieved by introducing the "variable" electron width $\gamma(\omega)$ into (7.1). This can be the universal (for all lines) function $\gamma(x)$ given by (2.20) and calculated from the adiabatic model. This gives reasonable agreement for the $Ly-\alpha$ line and the highly excited Balmer lines H_δ, H_8–H_{15} (see Figs. 11 and 15). More accurate results are also available for the $Ly-\alpha$ line, i.e., (6.15) (the nonadiabatic effects have also been taken into account[92,81]). We note that, in the wing, the line profile is satisfactorily described by (7.5) and (7.6).

The greatest computational difficulties are connected with the central part of the lines, where $\Delta\omega \ll \Delta\omega_0$, especially in the Balmer series. Detailed numerical calculations have recently been performed[84,85] both for this region and for the line as a whole. Vidal *et al.*[85] have reported numerical calculations for the first four Lyman lines ($Ly-\alpha$, $Ly-\beta$, $Ly-\gamma$, and $Ly-\delta$) and the four Balmer lines (H_α, H_β, H_γ, and H_δ) in a broad range of plasma densities and temperatures, i.e., N_e between 10^{11}–10^{12} and 10^{16}–10^{18} cm^{-3}; $T_e = T_i = 2500$ °K, 5000 °K, 10 000 °K, and 20 000 °K, and a broad range of wavelengths right up to line overlap.

The precision of these calculations is estimated[85] to be 10–15%. Precision of this order can probably be expected for the Lyman lines. However, in the case of the Balmer lines, the precision of the calculations is much lower. We have already noted the relatively considerable discrepancy between the data reported by Keple and Griem[84] and by Vidal *et al.*[85] near the centers of the H_α and H_γ lines. For the H_β and H_δ lines, the accuracy of the calculations at the center is also no better than 20%. However, it is important to note that the precision increases to 5–10% near the maximum and at moderate distances in the line wings (Figs. 7–10). The physical reasons restricting the accuracy of these calculations are, firstly, the thermal motion of the ions (Chap. 4) and, secondly, the nonuniformity of the plasma field (Chap. 10). The former group of effects leads to discrepancies between the true profile and the calculations near the line center, and these discrepancies increase with decreasing g_i. The second group affects the distant wings as well and, according to (10.7), is particularly important for highly excited lines in sufficiently dense plasma. We note that, in the distant line wings (especially for $Ly-\alpha$), the quantum-mechanical effects may become important for electrons.[78–81]

Summarizing, we may conclude that modern experiments have, on the whole, confirmed the basic predictions of the theory of Stark broadening of hydrogen lines. At the same time, the experimental results have presented new tasks for the theory, especially in relation to the accuracy of the calculated profiles within the framework of existing descriptions, and in the development of new approaches which may allow us to progress into a new range of plasma parameters. In the latter case, the most important problem is the development of a theory that would be valid for $g \sim 1$ throughout the line profile.

Finally, we note the existence of a detailed bibliography on line broadening.[104]

The author is greatly indebted to I. I. Sobel'man for encouragement in the writing of this review, to V. I. Kogan who read the manuscript and made several valuable suggestions, and to A. V. Demura and G. V. Sholin for discussions of many of the problems considered above.

[1]J. Holtsmark, Ann. Phys. (Leipzig) **58**, 577 (1919).
[2]D. Voslamber, Z. Naturforsch. Teil A **24**, 1458 (1969).
[3]E. W. Smith and C. F. Hooper, Phys. Rev. **157**, 126 (1967).
[4]E. W. Smith, Phys. Rev. **157**, 102 (1968).
[5]V. V. Yakimets, Zh. Eksp. Teor. Fiz. **51**, 1469 (1666) [Sov. Phys. JETP **24**, 990 (1967)].
[6]C. R. Vidal, J. Cooper, and E. W. Smith, J. Quant. Spectrosc. Radiat. Transfer **10**, 1011 (1970).
[7]R. Breene, The Shift and Shape of Spectral Lines, Pergamon, Press, New York (1961).
[8]H. R. Griem, Plasma Spectroscopy, McGraw-Hill, 1964 (Russ. Transl., Atomizdat, M., 1969).
[9]W. L. Wiese, in: Plasma Diagnostic Techniques, ed. by R. Huddlestone and S. L. Leonard (Russ. Transl., Mir, M., 1967, Chap. 6).

[10]I. I. Sobel'man, Vvedenie v teoriyu atomnykh spektrov (Introduction to the Theory of Atomic Spectra), Fizmatgiz, M., 1963 (English Transl., Pergamon Press, Oxford, 1972).
[11]M. Baranger, in: Atomic and Molecular Processes, ed. by D. R. Bates Academic Press, 1962 (Russ. Transl., Mir, M., 1964, Chap. 13).
[12]A. Traving, in: Plasma Diagnostics, ed. by W. Lochte-Holtgraven (Russ. Transl., Mir, M., 1971, Chap. 2).
[13]V. Weisskopf, Z. Phys. 25, 287 (1932).
[14]E. Lindholm, Arch. Mat. Astron. Fys. B 28, 1 (1942).
[15]L. D. Landau and E. M. Lifshitz, Kvantovaya mekhanika (Quantum Mechanics), Nauka, M., 1974 (English Transl., Pergamon Press, Oxford, 1975).
[16]P. W. Anderson, Phys. Rev. 86, 809 (1952).
[17]V. I. Kogan and V. S. Lisitsa, J. Quant. Spectrosc. Radiat. Transfer 12, 881 (1972).
[18]I. S. Gradshteĭn and I. M. Ryzhik, Tablitsy integralov, summ ryadov i proizvedeniĭ (Table of Integrals, Series and Products), Fizmatgiz, M., 1963 (English Transl., Academic Press, New York, 1966).
[19]V. S. Lisitsa, Dokl. Akad. Nauk SSSR 16, 1059 (1952).
[20]M. Lewis, Phys. Rev. 121, 501 (1962).
[21]V. I. Kogan, v kn. Fizika plazmy i problema upravlyaemykh termoyadernykh reaktsiĭ (in: Physics of Plasma and the Problem of Controlled Thermonuclear Reactions), ed. by M. A. Leontovich, Vol. 4, Izd. AN SSSR, M., 1958, p. 258.
[22]V. I. Kogan, Dokl. Akad. Nauk SSSR 135, 1374 (1960) [Sov. Phys. Dokl. 5, 1316 (1960)].
[23]S. D. Tvorogov and V. V. Fomin, Opt. Spektrosk. 30, 413 (1971) [Opt. Spectrosc. (USSR) 30, 228 (1971)].
[24]A. V. Demura and V. S. Lisitsa, J. Quant. Spectrosc. Radiat. Transfer 14, 273 (1974).
[25]H. Margenau and B. E. Meyerott, Astrophys. J. 121, 194 (1955).
[26]I. I. Sobel'man, Opt. Spektrosk. 1, 617 (1956).
[27]M. Baranger, Phys. Rev. 111, 481, 494; 112, 855 (1958).
[28]A. Jablonski, Phys. Rev. 68, 78 (1945).
[29]J. Szudy, Acta Phys. Pol. A 40, 361 (1971).
[30]J. Szudy and W. E. Bailis, J. Quant. Spectrosc. Radiat. Transfer 15, 641 (1975).
[31]L. A. Vaĭnshteĭn, L. V. Presnyakov, and I. I. Sobel'man, Zh. Eksp. Teor. Fiz. 43, 518 (1962) [Sov. Phys. JETP 16, 370 (1963)].
[32]S. Chandrasekhar, Stochastic Problems in Pyysics and Astronomy Rev. Mod. Phys. 15, 1 (1943) (Russ. Transl., IL, M., 1947).
[33]S. M. Rytov, Vvedenie v statisticheskuyu radiofiziku (Introduction to Statistical Radiophysics), Nauka, M., 1966.
[34]A. B. Underhill and J. Waddell, NBS Circ. No. 603 (1959).
[35]H. R. Griem, Astrophys. J. 132, 883 (1960).
[36]C. F. Hooper Jr., Phys. Rev. 165, 215 (1968).
[37]G. Ecker, Z. Phys. 148, 593 (1957).
[38]B. Mozer and M. Baranger, Phys. Rev. 118, 626 (1960).
[39]V. N. Alyamovskiĭ, Zh. Eksp. Teor. Fiz. 42, 1536 (1962) [Sov. Phys. JETP 15, 1067 (1962)].
[40]L. P. Kudrin, Statisticheskaya fizika plazmy (Statistical Physics of Plasma), Atomizdat, M., 1973.
[41]V. I. Kogan and A. D. Selidovkin, Plasma Phys. 9, 199 (1969).
[42]W. Pauli, Papers on Quantum Theory (Russ. Transl., Nauka, M., 1975, p. 99).
[43]T. Holstein, Phys. Rev. 79, 744 (1950).
[44]H. K. Wimmel, J. Quant. Spectrosc. Radiat. Transfer 1, 1 (1961).
[45]G. V. Sholin, V. S. Lisitsa, and V. I. Kogan, Zh. Eksp. Teor. Fiz. 59, 1390 (1970) [Sov. Phys. JETP 32, 758 (1971)].
[46]L. D. Landau and E. M. Lifshitz, Teoriya polya (Field Theory), Fizmatgiz, M., 1962 (English Transl. Pergamon, Oxford, 1976).
[47]H. R. Griem, A. C. Kolb, and K. Y. Shen, Phys. Rev. 116, 4 (1959).
[48]L. A. Vaĭnshteĭn and I. I. Sobel'man, Opt. Spektrosk. 6, 37 (1959) [Opt. Spectrosc. (USSR) 6, 279 (1959)].
[49]H. R. Griem, M. Baranger, A. C. Kolb, and G. Oertel, Phys. Rev. 125, 177 (1962).
[50]C. Deutsch, L. Herman, and H. W. Drawin, Phys. Rev. 178, 261 (1968).
[51]G. V. Sholin, A. V. Demura, and V. S. Lisitsa, Zh. Eksp. Teor. Fiz. 64, 2097 (1973) [Sov. Phys. JETP 37, 1057 (1973)].
[52]H. Pfennig, Phys. Lett. A 34, 292 (1971).
[53]L. A. Minaeva and I. I. Sobelman, J. Quant. Spectrosc. Radiat. Transfer 8, 783 (1968).
[54]M. L. Strekalov and A. I. Burshteĭn, Zh. Eksp. Teor. Fiz. 61, 101 (1971) [Sov. Phys. JETP 34, 53 (1972)].
[55]H. Pfennig, Z. Naturforsch. Teil A 26, 1071 (1971).
[56]L. Spitzer, Phys. Rev. 58, 348 (1940).
[57]M. I. Chibisov, Opt. Spektrosk. 27, 9 (1969) [Opt. Spectrosc. (USSR) 27, 4 (1969)].
[58]M. J. Seaton, Proc. Phys. Soc. London 77, 174 (1961).
[59]H. Pfennig, J. Quant. Spectrosc. Radiat. Transfer 12, 821 (1972).
[60]V. S. Lisitsa and G. V. Sholin, Zh. Eksp. Teor. Fiz. 61, 921 (1971) [Sov. Phys. JETP 34, 484 (1972)].
[61]M. Born, Lectures on Atomic Mechanics (Russ. Transl., ONTI, M., 1934).
[62]Yu. N. Demkov, B. S. Monozon, and V. N. Ostrovskiĭ, Zh. Eksp. Teor. Fiz. 57, 1431 (1969) [Sov. Phys. JETP 30, 775 (1970)].
[63]Yu. N. Demkov, V. N. Ostrovskiĭ, and E. A. Solov'ev, Zh. Eksp. Teor. Fiz. 66, 125 (1974) [Sov. Phys. JETP 39, 57 (1974)].
[64]V. N. Ostrovskiĭ and E. A. Solov'ev, Zh. Eksp. Teor. Fiz. 66, 1590 (1974) [Sov. Phys. JETP 39, 779 (1974)].
[65]T. Ishimura, J. Phys. Soc. Jpn. 23, 422 (1967).
[66]V. S. Lisitsa, Opt. Spectrosk. 31, 862 (1971) [Opt. Spectrosc. (USSR) 31, 468 (1971)].
[67]A. V. Demura, V. S. Lisitsa, and G. V. Sholin, in: Proc. Twelfth Intern. Conf. on Phenomena of Ionized Gases, Eindhoven, The Netherlands, 1975.
[68]L. P. Kudrin and G. V. Sholin, Dokl. Akad. Nauk SSSR 197, 342 (1962) [Sov. Phys. Dokl. 7, 1015 (1963)].
[69]V. I. Kogan, V. S. Lisitsa, and A. D. Selidovkin, in: Proc. Eighth Intern. Conf. on Phenomena on Ionized Gases, IAEA, Vienna, 1967.
[70]V. I. Kogan and V. S. Lisitsa, in: Proc. Ninth Intern. Conf. on Phenomena of Ionized Gases, IAEA, Bucharest, 1969.
[71]A. V. Demura, V. S. Lisitsa, and G. V. Sholin, Zh. Eksp. Teor. Fiz. 73, 400 (1977) [Sov. Phys. JETP 46, No. 2 (1977)].
[72]H. Margenau and M. Lewis, Rev. Mod. Phys. 31, 569 (1959).
[73]A. V. Vinogradov, I. I. Sobel'man, and E. A. Yukov, Kvantovaya élektronika (Moscow) 1, 268 (1974) [Sov. J. Qaunt. Electr. 4, 149 (1974)].
[74]R. L. Gree, J. Cooper, and E. W. Smith, J. Quant. Spectrosc. Radiat. Transfer 15, 1025 (1975).
[75]R. L. Green and J. Cooper, J. Quant. Spectrosc. Radiat. Transfer 15, 1037 (1975).
[76]H. R. Griem and K. Y. Shen, Phys. Rev. 122, 1490 (1961).
[77]V. A. Abramov and V. S. Lisitsa, Fiz. Plazmy 3(3) (1977).
[78]N. Tran Minh and H. Van Regemorter, J. Phys. B 5, 903 (1972).
[79]N. Tran Minh, N. Feautrier, and H. Van Regemorter, J. Phys. B 8, 1810 (1975); 9, 1871 (1976).
[80]N. Tran Minh, N. Feautrier, and H. Van Regemorter, J. Quant. Spectrosc. Radiat. Transfer 16, 849 (1976).
[81]F. F. Baryshnikov and V. S. Lisitsa, Zh. Eksp. Teor. Fiz. 72, 1797 (1977) [Sov. Phys. JETP 45, in press (1977)].
[82]N. F. Mott and H. S. Massey, Theory of Atomic Collisions, Oxford University Press, 1965 (Russ. Transl., Mir, M., 1969).
[83]A. Hautot, J. Math. Phys. 14, 1320 (1973).

[84]P. Keple and H. R. Griem, Phys. Rev. 123, 317 (1968).
[85]C. R. Vidal, J. Cooper, and E. W. Smith, Astrophys. J. Suppl. 25, 37 (1973).
[86]W. L. Wiese, D. E. Kelleher, and D. R. Paquette, Phys. Rev. 6, 1132 (1972).
[87]G. Boldt and W. B. Cooper, Z. Naturforsch. Teil A 19, 968 (1964).
[88]R. C. Elton and H. R. Griem, Phys. Rev. A 135, 1550 (1964).
[89]H. Schlütter and C. Avila, Astrophys. J. 144, 785 (1966).
[90]H. Schlütter, J. Quant. Spectrosc. Radiat. Transfer 185, 140 (1969).
[91]E. W. Smith, J. Cooper, and C. R. Vidal, Phys. Rev. 185, 140 (1969).
[92]V. S. Lisitsa and G. V. Sholin, J. Quant. Spectrosc. Radiat. Transfer 12, 985 (1972).
[93]D. E. Kelleher and W. L. Wiese, Phys. Rev. Lett. 31, 1431 (1973).
[94]W. L. Wiese, D. E. Kelleher, and V. Helbig, Phys. Rev. A 11, 1854 (1975).
[95]J. D. Hey and H. R. Griem, Phys. Rev. A 12, 169 (1975).
[96]H. W. Lee, P. Phys. B 6, 1060 (1973).
[97]J. Cooper, E. Smith, and C. R. Vidal, J. Phys. B 7, 101 (1974).
[98]E. Segre and D. Voslamber, Phys. Lett. A 46, 397 (1974).
[99]G. V. Sholin, Opt. Spektrosk. 26, 289 (1969) [Opt. Spectrosc. (USSR) 26, 155 (1969)].
[100]K. G. Müller, J. Quant. Spectrosc. Radiat. Transfer 5, 403 (1965).
[101]A. V. Demura and G. V. Sholin, J. Quant. Spectrosc. Radiat. Transfer 15, 881 (1975).
[102]A. Ts. Gurovich, L. K. Merenkova, and V. S. Éngel'sht, Dokl. Akad. Nauk SSSR 221, 315 (1975) [Sov. Phys. Dokl. 20, 200 (1975)].
[103]H. A. Bethe and E. E. Salpeter, Quantum Mechanics of One and Two Electron Atoms, Springer–Verlag, Berlin, 1957 (Russ. Transl., Fizmatgiz., M., 1960).
[104]NBS Special Publication 336, 1972 (Suppl. I—1973, Suppl. II—1975).

Translated by S. Chomet